



Optimal Demand Response Scheduling with Real Time Thermal Ratings of Overhead Lines for Improved Network Reliability

DOI:

[10.1109/TSG.2016.2542922](https://doi.org/10.1109/TSG.2016.2542922)

Document Version

Proof

[Link to publication record in Manchester Research Explorer](#)

Citation for published version (APA):

Kopsidas, K., Kapetanaki, A., & Levi, V. (2016). Optimal Demand Response Scheduling with Real Time Thermal Ratings of Overhead Lines for Improved Network Reliability. *IEEE Transactions on Smart Grid*, (99), 1-13. [DOI 10.1109/TSG.2016.2542922]. <https://doi.org/10.1109/TSG.2016.2542922>

Published in:

IEEE Transactions on Smart Grid

Citing this paper

Please note that where the full-text provided on Manchester Research Explorer is the Author Accepted Manuscript or Proof version this may differ from the final Published version. If citing, it is advised that you check and use the publisher's definitive version.

General rights

Copyright and moral rights for the publications made accessible in the Research Explorer are retained by the authors and/or other copyright owners and it is a condition of accessing publications that users recognise and abide by the legal requirements associated with these rights.

Takedown policy

If you believe that this document breaches copyright please refer to the University of Manchester's Takedown Procedures [<http://man.ac.uk/04Y6Bo>] or contact uml.scholarlycommunications@manchester.ac.uk providing relevant details, so we can investigate your claim.



Optimal Demand Response Scheduling With Real-Time Thermal Ratings of Overhead Lines for Improved Network Reliability

Konstantinos Kopsidas, *Member, IEEE*, Alexandra Kapetanaki, *Student Member, IEEE*, and Victor Levi, *Senior Member, IEEE*

Abstract—This paper proposes a probabilistic framework for optimal demand response scheduling in the day-ahead planning of transmission networks. Optimal load reduction plans are determined from network security requirements, physical characteristics of various customer types, and by recognizing two types of reductions, voluntary and involuntary. Ranking of both load reduction categories is based on their values and expected outage durations, while sizing takes into account the inherent probabilistic components. The optimal schedule of load recovery is then found by optimizing the customers' position in the joint energy and reserve market, while considering several operational and demand response constraints. The developed methodology is incorporated in the sequential Monte Carlo simulation procedure and tested on several IEEE networks. Here, the overhead lines are modeled with the aid of either static-seasonal or real-time thermal ratings. Wind generating units are also connected to the network in order to model wind uncertainty. The results show that the proposed demand response scheduling improves both reliability and economic indices, particularly when emergency energy prices drive the load recovery.

Index Terms—Optimal demand response, reliability, sequential Monte-Carlo, real time thermal rating, risk.

NOMENCLATURE

The symbols used throughout this paper are defined below.

Indices

j	Index of generating units running from 1 to J
i	Index of load points running from 1 to N
s	Index of load types running from 1 to s_4
t	Index of hours running from 1 to T
y	Index of simulation days running from 1 to Y.

Parameters

$VOLL_i^s$	Value of lost load at load point i and load type s
------------	--

Manuscript received April 26, 2015; revised August 22, 2015 and November 27, 2015; accepted March 6, 2016. This work was supported by the Engineering and Physical Sciences Research Council within the HubNet Project under Grant EP/I013636/1. Paper no. TSG-00463-2015.

The authors are with the School of Electrical and Electronic Engineering, Electrical Energy and Power Systems Group, University of Manchester, Manchester M13 9PL, U.K. (email: k.kopsidas@manchester.ac.uk; alexandra.kapetanaki@manchester.ac.uk; victor.levi@manchester.ac.uk).

Color versions of one or more of the figures in this paper are available online at <http://ieeexplore.ieee.org>.

Digital Object Identifier 10.1109/TSG.2016.2542922

$\hat{B}EDI_i$	Normalized value of expected duration interruption index in the base case	34
D_i^s BASE	Duration of interruption of load type s at load point i under the base case	35
P_g^{\max}	Maximum power output of a generation unit	36
P_g^{\min}	Minimum power output of a generation unit	37
P_d^{\max}	Maximum forecast load	38
$VL_i^{s,\max}$	Upper limit of the voluntary load reduction for customer type s	39
$IVL_i^{s,\max}$	Upper limit of the involuntary load reduction for customer type s	40
B	System matrix including potential contingencies	41
win	Per unit window for load reduction sampling	42
rs	Random number between $\{0,1\}$	43
t_{MAX}	Maximum hour limit of load recovery	44
f_{REC}^s	Customer's availability to recover the load	45
V_{ci}	Cut in wind speed	46
V_r	Rated wind speed	47
V_{co}	Cut out wind speed	48
P_r	Rated power output of wind turbine	49
$T_c(t)$	Conductor temperature at hour t	50
$R(t)$	AC conductor resistance at operating temperature T_c at hour t	51
$P_c(t)$	Convection heat loss at hour t	52
$P_r(t)$	Radiated heat loss at hour t	53
$P_s(t)$	Solar heat gain at hour t	54
$I(t)$	Conductor current at hour t	55
$V_m(t)$	Wind speed at hour t	56
$K_{angle}(t)$	Wind direction at hour t	57
$T_a(t)$	Ambient temperature at hour t .	58

Variables

$P_{g_j}(t)$	Active Power output of generation unit j at hour t	59
θ	Phase angles of nodal voltages	60
$\mu_i(t)$	Nodal marginal price of load point i at hour t	61
$\gamma_i^s(t)$	Slope coefficient for load recovery at node i , type s , hour t	62
P_f^{\max}	Overhead line real-time thermal rating	63
$P_{di}(t)$	Power supplied to load point i at hour t	64
$\sigma_i^s(t)$	Marginal offer value for voluntary load reduction, load type s at load point i at hour t	65

76	$VL_i^s(t)$	Amount of voluntary load reduction of load type s at load point i at hour t
77		
78	$IVL_i^s(t)$	Amount of involuntary load reduction of load type s at load point i at hour t
79		
80	$D_i^s(t)$	Duration of interruption of load type s at load point i at hour t
81		
82	$Pc_i^s(t)$	Total load shedding of load type s at load point i at hour t
83		
84	$f_{RED}^s(t)$	Load type s availability to respond to a demand response call at hour t
85		
86	$CVL_i^s(t)$	Contracted voluntary load reduction of load type s at load point i at hour t .
87		

88 Functions

89	$GR_j(\cdot)$	Revenue of generator j
90	$LC_i(\cdot)$	Cost of delivered demand at node i
91	$VLR_i(\cdot)$	Revenue for voluntary load type s reduction at node i
92		
93	$IVLR_i(\cdot)$	Revenue for involuntary load type s reduction at node i
94		
95	$\hat{R}_i^s(\cdot)$	Ranking order for load type s at node i
96	$[\Lambda^-]_i^s(\cdot)$	Size of load reduction for load point i type s
97	$[\Lambda^+]_i^s(\cdot)$	Size of load recovery for load point i type s
98	$Savings_i^s(\cdot)$	Customer savings for load point i type s in the event that demand response materializes
99		
100	$C_{payback}^s i(\cdot)$	Payback cost due to load recovery at node i type s
101		
102	$\pi_i^s(\cdot)$	Profit of load customer at load point i type s
103	$VaR_\alpha^{NR}(\cdot)$	Value at risk for network rewards at confidence level α
104		
105	$VaR_{1-\alpha}^{NC}$	Value at risk for network costs at confidence level $1-\alpha$
106		
107	$P(\cdot)$	Wind turbine power output for wind speed V_m .

108 I. INTRODUCTION

109 **T**HE EVER increasing integration of intermittent renewable energy into the electricity network, combined with
 110 a constantly growing demand, is likely to cause much greater
 111 stress on existing networks increasing the probability of
 112 severe contingencies [1]. To avoid this, several preventive and
 113 corrective actions, including demand response (DR), spinning
 114 reserve scheduling, application of real-time thermal ratings
 115 (RTTR) and energy storage scheduling, can be deployed
 116 to relieve stress in particular areas of the network.

117 DR strategies currently under investigation consider distribution level [2], [3], but their potential in transmission
 118 networks is often overlooked. Research related to the impact
 119 of DR on network reliability is very limited [4]–[6]. The
 120 model proposed in [5] evaluates short term operational benefits
 121 in terms of generation and interrupted energy costs from
 122 interruptible loads by using the contingency enumeration
 123 technique; however, it does not fully address the customer
 124 perspective because there is no modelling of load recovery and
 125 associated costs, characteristics of different load and DR types
 126 and probabilistic nature of available interruptible demand.
 127 Even if a probabilistic approach is used to assess the DR
 128 contribution [6], only single contingencies are analysed.

Physical characteristics of different types of load customers
 need to be adequately represented in the studies. Domestic
 and small commercial loads are analysed in [7]–[9] but fail to
 assess how critical each customer type is for a network's load
 point in terms of interruptions. Next, examining different sizes
 and shapes of both load reduction and recovery is essential for
 a complete and accurate network assessment; however, load
 recovery is usually ignored in the studies [4]. Load reduction
 and recovery can be based on electricity market prices in order
 to eliminate price spikes during peak hours [4], [10]. However,
 these studies often ignore operational and security constraints
 of the transmission networks and are run for intact networks
 only. Enumeration techniques, as opposed to Monte Carlo simulation,
 are often used to calculate the DR contribution, and thus fail to
 include the whole set of contingencies and a number of uncertainties
 a network might experience [11]. Finally, instead of applying DR
 every time a contingency occurs, DR should only be used when the
 reliability is improved and when savings are higher than the expected
 payback costs.

This paper proposes a probabilistic approach for optimal demand
 response scheduling in the day-ahead planning of transmission
 networks. Uncertainties related to forecast load, network component
 availability, available amount of demand response and wind speeds
 are incorporated into the sequential Monte Carlo simulation
 framework. Synchronous and wind generating units, as well as
 four types of load customers (large, industrial, commercial and
 residential) are modelled. Optimal nodal load reductions are
 calculated using the optimum power flow model, and are then
 disaggregated into voluntary and involuntary components. Recognizing
 that directly-controlled loads can certainly be shed and indirectly-
 controlled contain a probabilistic component, optimal amounts of
 voluntary and involuntary nodal reductions are determined. Different
 load recovery profiles for customer types are considered next within
 'payback periods' and they are initiated when the load customer's
 revenue is highest. Here, delivered load is priced at nodal marginal
 price, voluntary load reduction at marginal offer price and involuntary
 load reduction at damage cost. The whole analysis is implemented
 from the load customer's perspective to maximise their revenues,
 whilst the load recoveries are controlled by the transmission system
 operator (TSO); they may represent either physical paybacks from
 specific appliances or controlled paybacks whereby the TSO
 schedules its customer loads so as to have the desired shape. The
 benefits of optimal DR strategies are evaluated in combination with
 real-time thermal ratings of overhead lines to reveal the true
 potential of the DR. The outputs of the model also include financial
 risk quantifiers that the revenues are below, or costs are above a
 threshold.

180 II. OVERVIEW OF THE METHODOLOGY

Optimal DR scheduling is determined using the sequential Monte Carlo
 probabilistic approach. The main features of the proposed DR modeling
 framework are: a) Load reduction scheduling driven by network security;
 b) Optimal scheduling of load recovery using economic criteria;
 c) Modelling of real-time thermal ratings of overhead lines;

187 and d) Modelling of renewable energy sources, such as wind
188 generation.

189 The overall methodology is realized within two independ-
190 ent sequential Monte Carlo simulation (SMCS) procedures.
191 The first SMCS is the initialization module, which is used to
192 calculate several components required by the second SMCS
193 that determines optimal day-ahead operation of the power sys-
194 tem. The main building blocks of the first SMCS procedure
195 are: a) Calculation of reliability indices needed for ranking
196 of load types for demand reduction; b) Calculation of real-
197 time thermal ratings of overhead lines; and c) Determination
198 of nodal marginal prices and several economic indicators used
199 for finding the optimal schedule of load recoveries.

200 The second SMCS consists of four modules: a) Demand
201 reduction scale module; b) Load recovery scale module;
202 c) Demand reduction and load recovery (DRLR) control mod-
203 ule, and d) The outputs module. The first module contains
204 ranking of different load types for demand reduction, calcu-
205 lation of required amounts of voluntary and involuntary DR,
206 as well as the customer revenues. The load recovery scale
207 module considers load recovery profiles and sizes, and deter-
208 mines a matrix with the most appropriate schedule hours for
209 load recovery. The DRLR-control module contains logics for
210 initiation of load reductions and load recoveries, whilst the
211 outputs module includes optimal load reduction and recovery
212 schedules, as well as reliability and financial indicators.

213 III. METHODOLOGY

214 The proposed demand scheduling methodology is aimed
215 at determining the optimal demand response plan for the
216 next day, when the committed generation units, status of net-
217 work switching devices and forecast loads are well defined.
218 However, several uncertainties in the day-ahead operation are
219 still present, so that the overall problem is formulated as
220 a probabilistic model and solved with the SMCS. The pro-
221 posed DR methodology is applied for post contingency states;
222 however it is general enough to also consider pre-contingency
223 events. The main building blocks are briefly presented below.

224 A. Sequential Monte Carlo Simulation

225 Sequential Monte Carlo simulation performs analysis of
226 time intervals in chronological order whilst taking into account
227 various uncertainties [11]. It can model the chronological
228 phenomena, such as load reduction and recovery, real-time
229 thermal ratings and wind generations. Following uncertainties
230 were assumed for a day-ahead operation of the transmission
231 network:

- 232 • Load varies in a window around the forecast hourly loads.
233 The uncertainty window is defined by the MAPE of the
234 short-term forecast by hourly intervals obtained using the
235 neural network approach [12].
- 236 • Availability of all generation and network units was mod-
237 elled with the aid of two-state Markovian model with
238 exponentially distributed up and down times [11].
- 239 • Wind speed hourly predictions and a window around the
240 predicted values are applied within the random sampling.

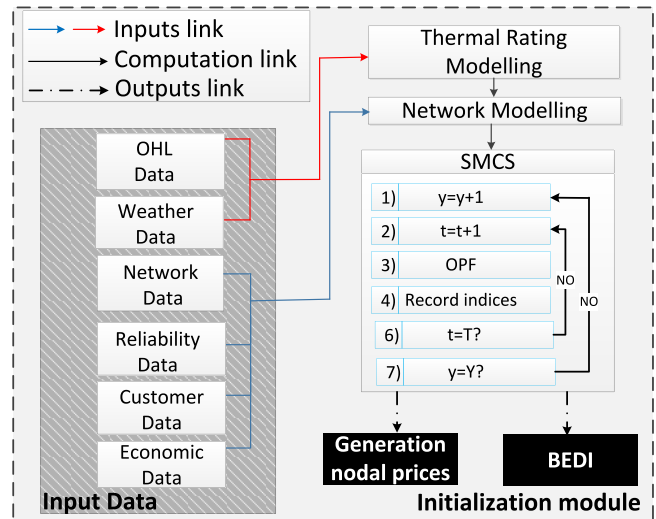


Fig. 1. Computations within the initialization module.

An alternative approach is to use wind speed probability
distribution functions (PDFs) by hourly periods.

- Amount of voluntary load reduction that varies by cus-
tomer and DR type. For example, DR from residential
customers responding to price signals is highly uncertain,
whilst DR from incentive-based contracted commercial
customers has much less uncertainty – see Section III-D.

One SMCS period is equal to 24 hours and simulations are
repeated until convergence is obtained. Any failure that goes
over the planning horizon (i.e., 24:00) was considered in the
'next day' simulation. The same simulation principles were
applied in both SMCS procedures.

253 B. Initialization Module

254 The initialization module is used to calculate several quan-
255 tities required by the main simulation loop. Following the
256 data input, network model with real-time thermal ratings and
257 load customer characteristics is built and fed into the first
258 SMCS procedure, as shown in Fig. 1. The outputs from this
259 stage are some pricing and reliability indicators.

1) *Input Data*: The input data include network, reliabil-
ity, customer, economic data, overhead line (OHL) data and
weather data. Beside the standard network data, forecast in-
service generation units with technical characteristics and
chronological hourly load point demands are input. Reliability
data are failure rates and repair times of all components, whilst
customer data encompass customer and DR types, contracted
voluntary load reductions, normalized load recovery profiles
and customer availability to respond to a DR call. Essential
economic data are generation costs, values of lost load (VOLL)
and marginal offer prices for voluntary load reduction. Average
VOLL data by customer types were obtained from the latest
U.K. national study [13].

Weather data include ambient temperatures, wind speeds
and directions required for the calculation of RTTRs of OHLs,
as well as either forecast hourly wind speeds or hourly wind
speed PDFs used to calculate wind generations. Several other

277 OHL construction and heat dissipation/gain data are further
278 required to calculate RTTRs.

279 The input data are fed into the thermal ratings and network
280 modelling modules, whose outputs are then used by the SMCS
281 procedures.

282 2) *Thermal Ratings of Overhead Lines*: Two different OHL
283 rating models are used in the developed simulation proce-
284 dures, the ‘seasonal’ thermal rating (STR) and the RTTR. The
285 STR is defined by seasons and for different design conductor
286 temperatures [14]. The lowest ratings are for summer con-
287 ditions and design temperature of 50°C [15]; they are of
288 conservative nature.

289 To get the RTTRs, it is possible to do a thermal analysis on
290 an hourly basis. Assuming a steady-state thermal equilibrium
291 is achieved in each hourly period, static thermal balance is
292 achieved by equating heat dissipated by convection and radi-
293 ation (or ‘cooling’) with solar and Joule heat generated. In
294 the applied IEEE model [15], the convection heat loss varies
295 with the change in wind speed (V_m), wind direction factor
296 (K_{angle}) and the difference between the conductor (T_c) and
297 ambient air temperature (T_a). The radiation heat loss is the
298 energy of the electromagnetic waves emitted to the ambient
299 space; it is a function of the temperature difference between
300 the conductor and air, and the emissivity of the conductor. The
301 solar radiation is a function of several parameters including
302 solar azimuth, total radiated heat flux rate, etc. Finally, Joule
303 (I^2R) losses are calculated in the standard way using AC resis-
304 tance dependent on conductor temperature, so that the RTTR
305 of OHLs is determined as:

$$306 \quad I = \sqrt{(P_c(T_c, T_a, K_{angle}, V_m) + P_r(T_a, T_c) - P_s) / R(T_c)} \quad (1)$$

307 where $P_c(\cdot)$ is the convection heat loss, $P_r(\cdot)$ is the radiated
308 heat loss, P_s is solar heat gain and $R(T_c)$ is the conductor
309 resistance at operating temperature T_c . The conductor temper-
310 ature needs to be set to one of the standard design values
311 (i.e., 50°C, or 65°C, or 75°C) to get the OHL ampacity; an
312 increased value can be used during system emergencies.

313 The average values of 5-year hourly weather data were
314 obtained from the BADC MIDAS meteorological stations for
315 Aonach, U.K. [16]. The rest of the required data were obtained
316 from the U.K. consultants.

317 3) *Analysis Within the SMCS Procedure*: The initialization
318 module is used for two purposes; the first is to determine
319 the base expected duration interruption (BEDI) index of loads
320 needed for ranking of loads within the demand reduction
321 scale module. The second is to compute the probabilistic
322 energy nodal prices used within the DRLR-control module
323 to find the optimal load recovery strategy. The probabilistic
324 nodal prices at different confidence intervals α are further
325 analysed to make decision about the most appropriate load
326 recovery times.

327 Each hour within the simulation period is characterized by
328 available generating units, transformers and circuits, as well
329 as nodal loads and operational constraints. An optimum power
330 flow (OPF) model is solved to find the levels of voluntary
331 and involuntary load reductions and revenues to generator
332 and demand customers. The formulation of the OPF model is
333 a modification of the market-clearing model proposed in [17];

the main difference is that there is no preventive control 334
and corrective scheduling is applied to the already sampled 335
contingent case. Mathematical formulation of the model is: 336

$$337 \quad \text{Min} \left\{ \sum_{j \in J} C_{gj} \cdot P_{gj} + \sum_{i \in I} \sum_{s \in S} VOLL_i^s \cdot IVL_i^s \right. \\ \left. + \sum_{i \in I} \sum_{s \in S} \sigma_i^s \cdot VL_i^s \right\} \quad (2) \quad 338$$

$$339 \quad \text{subject to: } P_g - P_d - B\theta = 0 \quad (\mu) \quad (3) \quad 339$$

$$340 \quad P_f = H\theta \quad (4) \quad 340$$

$$341 \quad -P_f^{\max} \leq P_f \leq P_f^{\max} \quad (5) \quad 341$$

$$342 \quad -P_g^{\min} \leq P_g \leq P_g^{\max} \quad (6) \quad 342$$

$$343 \quad 0 \leq VL_i^s \leq VL_i^{s, \max} \quad (7) \quad 343$$

$$344 \quad 0 \leq IVL_i^s \leq IVL_i^{s, \max} - VL_i^{s, \max} \quad (8) \quad 344$$

$$345 \quad P_d^{\max} - \sum_s IVL^s - \sum_s VL^s \leq P_d \leq P_d^{\max} \quad (9) \quad 345$$

346 The objective function to be minimized (2) is the sum of
347 the offered cost functions for generating power plus the sum
348 of the cost of involuntary load reduction for all load nodes
349 and types plus the sum of offered costs for voluntary load
350 reduction for all load nodes and types. The involuntary load
351 reduction is valued at $VOLL$ that is dependent on the general
352 load type; dependency on the connection node is taken into
353 account because there may exist special loads whose curtail-
354 ment must be avoided. Voluntary load reduction is priced at
355 the rates offered by consumers to provide this service. They
356 are closely linked to the offers made by generators for the ‘up-
357 spinning reserve’ in the joint energy and reserve market [17].
358 It is again envisaged that the rates can vary with customer
359 type and connection location. Finally, note that time index t
360 is avoided for simplicity.

361 Using a dc load flow model, constraints (3) represent the
362 nodal power balance equations for the considered state, which
363 includes potential contingencies within the system matrix B .
364 A Lagrange multiplier (or dual variable) μ_i is associated with
365 each of the equations. Constraints (4) express the branch flows
366 in terms of the nodal phase angles, while constraints (5)
367 enforce the corresponding branch flow capacity limits. Here,
368 modelling of OHL ratings can be done using the RTTR model,
369 in which case limit P_f^{\max} is a function of the time step t .

370 Constraints (6) set the generation limits for the consid-
371 ered state, while considering available units and requirements
372 for the down- and up-spinning reserve in the analysed time
373 step [17]. Reserve requirements depend on the system load and
374 contingency state [17]. For the non-controllable units, such as
375 wind turbines, upper and lower limits are the same.

376 Constraints (7), (8) and (9) set the limits of the demand; they
377 are expressed as inequality constraints on the voluntary and
378 involuntary load reductions and the total delivered load. The
379 upper limit of the voluntary load reduction $VL_i^{s, \max}$ can contain
380 a probabilistic component for some DR types and is dependent
381 on the considered time step. As a consequence, the upper limit
382 of the involuntary load reduction is the difference between of
383 the absolute limit $IVL_i^{s, \max}$ and the voluntary load reduction

384 limit $VL_i^{s,max}$. Finally, the delivered demand P_d is equal to
 385 the forecast load in the considered time interval P_d^{max} if there
 386 is no load reduction. The lower limit is specified in terms of
 387 the forecast load, voluntary and involuntary load reductions,
 388 which are a part of the optimal solution.

389 Solving the optimization model (2) to (9) gives the optimal
 390 values of the unknown variables, as well as dual variables
 391 associated with the constraints of this problem [18]. The
 392 significance of the dual variables is discussed below.

393 4) *Nodal Marginal Costs*: The optimal solution of the
 394 problem (2) to (9) is equal to the optimal solution of the cor-
 395 responding dual problem whose unknowns are dual variables
 396 associated with the constraints (3) to (9) [18]. The objective
 397 function of the dual problem is a sum of products of the dual
 398 variables and the right-hand sides of the constraints, showing
 399 that the total optimal cost can be recovered in another way
 400 using the dual variables as charging rates. The dual variables
 401 represent the additional cost of changing the right-hand side
 402 of the constraints by unity; they are therefore called marginal
 403 costs or prices [19].

404 Dual variables μ are the nodal marginal costs of meeting the
 405 power balance at each system node for the considered oper-
 406 ating regime. The nodal marginal costs have been extensively
 407 used for electricity energy and reserve pricing [6], [9], [20].
 408 The nodal marginal prices vary over the system nodes and
 409 during the day due to load variation and congestion in the
 410 system [21]. The greatest variation of marginal prices is
 411 experienced due to unexpected failures of lines and/or gener-
 412 ator units [6]. Consequently, these prices should be carefully
 413 considered for the load recovery scheduling.

414 In our approach, we have applied a concept similar to
 415 the real time pricing scheme proposed in [22]. The following
 416 quantities are calculated in each time step t :

- 417 • The revenue of generator j :

$$418 \quad GR_j(t) = Pg_j(t) \cdot \mu_j(t) \quad (10)$$

- 419 • The cost of demand i delivery:

$$420 \quad LC_i(t) = P_{di}(t) \cdot \mu_i(t) \quad (11)$$

- 421 • Revenue for voluntary load i reduction:

$$422 \quad VLR_i(t) = \sum_{s=1}^{s4} (\sigma_i^s(t) \cdot VL_i^s(t)) \quad (12)$$

- 423 • Revenue for involuntary load i reduction:

$$424 \quad IVLR_i(t) = \sum_{s=1}^{s4} (VOLL_i^s \cdot IVL_i^s(t)) \quad (13)$$

425 We have defined $VOLL$ by load types in the initialization mod-
 426 ule, as presented in equation (13). However, in the second
 427 SMCS there is an option to use a look-up table where $VOLLs$
 428 are functions of interruption duration [23]. The interruption
 429 duration is estimated as:

$$430 \quad D_i^s = \begin{cases} \text{mean}(D_i^s \text{ BASE}), & \text{if } D_i^s \leq \text{mean}(D_i^s \text{ BASE}) \\ D_i^s, & \text{if } D_i^s > \text{mean}(D_i^s \text{ BASE}) \end{cases} \quad (14)$$

431 where $D_i^s \text{ BASE}$ denotes the interruption duration calculated
 432 in the initialization module. The estimated duration of

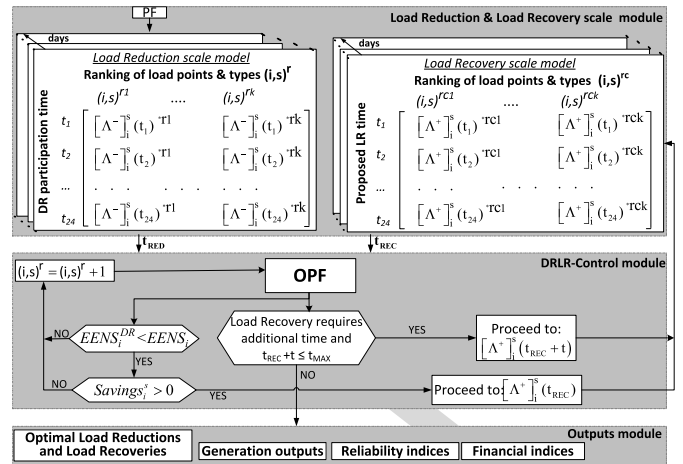


Fig. 2. Optimal demand response computational framework.

433 interruption is equal to the mean base value unless the inter-
 434 ruption already lasts for more than the base value; it then takes
 435 the actual duration value.

436 C. Optimal Demand Response Scheduling

437 The computational framework for optimal demand response
 438 scheduling is illustrated in Fig. 2. The load reduction and
 439 recovery scale modules feed into the DRLR control module.
 440 Ranking of different load types and calculation of *available*
 441 sizes for voluntary load reduction is performed within the load
 442 reduction scale module. The order of ranking the load points
 443 and types is represented by $(i, s)^r$ in Fig. 2. Hence, in the load
 444 reduction matrix, if load reduction takes places at hour t_j the
 445 load reduction of $(i, s)^r$ customer will be evaluated first, while
 446 the $(i, s)^{rk}$ customer will be evaluated at the end.

447 The load recovery scale module computes the most appro-
 448 priate schedule hours for load recovery, as well as the potential
 449 recovery sizes and profiles. The order of ranking the load
 450 points and types is represented by $(i, s)^c$ in Fig. 2. Hence, in
 451 the load recovery matrix, if load recovery takes places at hour
 452 t_j the load reduction of $(i, s)^{rc1}$ customer will be evaluated
 453 first, while the $(i, s)^{rck}$ customer will be evaluated at the end.
 454 Both load reduction and recovery are managed by the DRLR
 455 control module in which the OPF is used to determine optimal
 456 voluntary and involuntary load reductions, and the developed
 457 control scheme gives the optimal load recovery profiles. The
 458 outputs module finally gives optimal DR and LR schedules,
 459 as well as financial and reliability indicators.

460 D. Load Reduction Scale Module

461 Load reduction scale module is required for each load point
 462 and load type when load shedding takes place at the considered
 463 hour t_{RED} . The physics of demand response are presented first,
 464 which is followed by the ranking and sizing.

465 Four load types, industrial, commercial, large user and
 466 residential, have been defined in our approach. Different
 467 characteristics have been associated with these four types,
 468 such as temporal load variations, total amounts available for

voluntary and involuntary load reductions, relative load recovery profiles and economic data. Two categories of demand response have been recognised, namely direct and indirect load control [24]. In direct load control, the contracted customers (usually large and industrial) are directly disconnected during emergency conditions and they receive revenue for participating in the ‘reserve market’ [25]. The contracted amounts are certain and they are of deterministic nature. In indirect load control, incentive- and price-based demand responses can be distinguished. The former group refers to the customers contractually incentivised to curtail load during system emergencies [26], [27]. This category can be considered semi-probabilistic; we have used sampling within a window around the contracted value. Finally, in price based demand response customers move their consumption from periods of higher to periods of lower prices. This demand response is a probabilistic quantity which can vary from zero up to the estimated maximum amount.

Load ranking at each node i and for each load type s at the considered hour t_{RED} is based on the financial implications of reducing the load. The ranking order is a product of the normalized value of the base expected duration interruption index ($BEDI_i$) calculated in the initialization module, the normalized marginal offer price $\hat{\sigma}_i^s$ for voluntary load reduction or customer interruption cost $VOLL_i^s$ for involuntary load reduction, and the required load shedding Pc_i^s . This is shown in relations below:

$$\hat{R}_i^s(t_{RED}) = \begin{cases} \hat{B}EDI_i \cdot Pc_i^s \cdot \hat{\sigma}_i^s, & \text{voluntary load} \\ \hat{B}EDI_i \cdot Pc_i^s \cdot VOLL_i^s, & \text{involuntary load} \end{cases} \quad (15)$$

$$BEDI_i = \sum_{y=1}^Y \sum_{t=1}^T \sum_{s=1}^{s_4} \zeta_i^s \cdot D_i^{BASE} / Y \quad (16)$$

Relation (15) shows that independent ranking lists for voluntary and involuntary load reductions can be built. Ranking of all ‘voluntary customers’ is based on submitted marginal offer prices, which can be normalised with the average price of up-spinning reserve in the energy-reserve markets [17]. On the other hand, involuntary load reductions are ranked using $VOLL$. The $VOLL$ is defined either by load types, or customer damage functions are used; it is normalised using the average $VOLL$ in the entire GB [13]. The base expected interruption index $BEDI_i$ is found from the number of interruptions ζ_i^s having duration D_i^{BASE} across the entire simulation period.

The total required amount of load reduction Pc_i^s is determined from the OPF model and it consists of voluntary and involuntary components. When considering industrial and large customers under the direct load control, it was assumed that available voluntary load reduction is equal to the contracted voluntary reduction (CVL_i^s). Then the (part of) voluntary load reduction is:

$$[\Lambda^-]_i^s(t_{RED}) = \begin{cases} Pc_i^s(t), & \text{if } Pc_i^s(t) < CVL_i^s(t) \\ CVL_i^s(t), & \text{if } Pc_i^s(t) > CVL_i^s(t) \end{cases} \quad (17)$$

Available voluntary load reductions from industrial and commercial incentivised customers and residential customers contain a probabilistic component that can be determined using random sampling. It is calculated using the availability

factor f_{RED}^s :

$$f_{RED}^s = \begin{cases} 1 + (rs - 1)win, & \text{industrial \& commercial} \\ rs, & \text{domestic customers} \end{cases} \quad (18)$$

where rs is a random number generated from the uniform distribution between $\{0,1\}$ and win is the per unit window. In case of incentivised (industrial and commercial) customers, the available amount is based on average probability that the contracted amount is available; for example, if the probability is 0.9 then $win=0.2$. Residential customers respond to price signals and the uncertainty window is the entire available range. The available voluntary load reduction is then calculated by multiplying the availability factor (18) and the contracted value (CVL_i^s) in case of incentivised industrial and commercial customers, or estimated maximum load reduction of residential customers.

After having obtained *available* voluntary load reductions for all types of customers s at node i , the total voluntary and involuntary load reductions are calculated using the ranking order and a relation similar to expression (17). The minimum amount of involuntary load reduction is always used to meet the network security constraints.

E. Load Recovery Scale Module

This module determines the amounts of *potential* load recoveries in the period following load reduction in time slot t_{RED} . The actual load recovery is determined in the DRLR control module using the hourly nodal marginal prices.

Load recovery profiles can be very different for the considered customer types, and moreover, for different customers within a single group; a good example is industry [28]. We applied a general normalized load recovery profile of triangular shape, which is modelled by two straight lines in discrete form. The upward line models load pick-up after the customer reconnection, whilst the downward line brings it back from the ‘overshot point’ to the pre-disconnection value. The discrete modelling is done using the upward/downward slope coefficients in consecutive time intervals.

The amount of load recovery at time period $t_{REC} + t$, $[\Lambda^+]_i^s(t_{REC} + t)$, is computed by using the following expression:

$$[\Lambda^+]_i^s(t_{REC} + t) = [\Lambda^-]_i^s(t_{RED}) \cdot \gamma_i^s(t_{REC} + t) \cdot f_{REC}^s \quad (19)$$

where $[\Lambda^-]_i^s(t_{RED})$ is amount of load reduction of load type s at node i , $\gamma_i^s(t_{REC} + t)$ is upward or downward slope coefficient and f_{REC}^s is the availability factor of type s load recovery. This factor was introduced because not all customers may come back when supplies are restored or signalled [29]. In the current approach, availability factors f_{REC} are deterministic quantities defined by customer types and network nodes. It is also worth noting that the load recovery can be higher than the amount of the initial load reduction [28]; the slope factors can take values greater than unity.

Modelling of load recovery profiles over a specified time period introduces additional complexities in the developed SMCS methodology. Each time a load recovery is initiated, the corresponding nodal load needs to be modified over a specified

574 period in line with the load recovery profile. Besides, a record
575 must be kept of all load recoveries at different time steps,
576 because they cannot be considered for further load reduction.
577 This is reflected in the next DRLR module.

578 F. Demand Reduction Load Recovery Control Module

579 The DRLR control module is used to control the initiation
580 of load reductions and recoveries and to produce their optimal
581 schedules within the forecast 24 hourly period. Some of the
582 control principles are listed below:

- 583 • Loads whose recovery process is underway cannot be
584 considered for load reduction.
- 585 • Loads eligible for load reduction will not be disconnected
586 if there is no improvement in the energy-not-served
587 following the load reduction.
- 588 • Only those loads, whose reduction including recovery
589 generates revenue to the customers, will be actually
590 disconnected and reconnected.
- 591 • The best timing of load recovery is determined using
592 the (forecast) nodal marginal prices over the recovery
593 period.

594 Assume the OPF analysis has generated non-zero load cur-
595 tailments. Those loads which are not a part of previous load
596 recoveries are ranked and sizes of voluntary and involuntary
597 reductions are determined. The first load reduction from the
598 ranking list is applied and it is checked with the aid of the
599 OPF whether the total energy-not-served has reduced. If this
600 is the case, the nodal customer *profits* are computed based on
601 the *savings* acquired due to the load reduction and the pro-
602 jected *payback cost* due to the load recovery. The optimum
603 load recovery always takes place when the nodal marginal
604 prices are ‘low’ over the recovery window. If the load cus-
605 tomer projected profit is negative, the load reduction is not
606 activated even if the reliability of the network might improve.

607 Calculation of customer savings, costs and profits is briefly
608 presented below.

609 1) *Customer Savings*: The customer savings incurred dur-
610 ing load reduction are the consequence of reduced load
611 payments to the generators. These payments are valued at
612 nodal marginal prices $\mu_i(t)$, as shown in equation (11), which
613 are in turn dependent on the considered regime. The customer
614 savings are therefore calculated from two OPF runs: the first
615 without load reduction and the second with load reduction.
616 The change in load payments, ΔLC , represents the customer
617 savings at t_{RED} :

$$618 \quad \Delta LC_i^s(t_{RED}) = LC_i^{s\ NO-DR}(t_{RED}) - LC_i^{s\ DR}(t_{RED}) \quad (20)$$

619 The total savings are then found for the entire interval when
620 the load reduction is in place:

$$621 \quad Savings_i^s(t_{RED}) = \sum_{t=t_{RED}}^{t_{REC}} \Delta LC_i^s(t) \quad (21)$$

622 2) *Payback Costs*: If customer *savings* are positive then the
623 algorithm proceeds to the load recovery stage to project the
624 optimal load recovery schedule. The optimization is based on
625 the following principles:

- Load recovery is always scheduled after the correspond- 626
ing load reduction and it can continue into the ‘following’ 627
simulated day. There are periods within a day when the 628
load recovery does not take place; for example between 629
12am and 5pm on weekdays for residential customers. 630
- Load recovery blocks due to involuntary load reduction 631
are always committed before voluntary load recovery 632
blocks. They are prioritized based on their VOLL; where 633
the VOLL is the same, ranking is based on the size of 634
load reduction, the largest loads being reconnected first. 635
Similar criteria are applied to voluntary load reductions, 636
where marginal offer prices are used instead of VOLL. 637
- Optimal timing of load recovery is determined by find- 638
ing the weighted average of (base) nodal marginal prices 639
over the recovery window. The weights are equal to the 640
slope coefficients $\gamma_i^s(t_{REC} + t)$ of the normalized recov- 641
ery profile. The window with the smallest average nodal 642
marginal price is selected for the load recovery. This 643
approach is the best for load customers, because they 644
will be exposed to the least additional payback cost. 645
- After having determined the optimal starting hour of load 646
recovery, it will only be materialized if there will be no 647
new load curtailments within the recovery window. This 648
is checked by running OPF over consecutive time periods 649
within the recovery window; where curtailments occur, 650
the next best recovery window is examined and so on. 651

The payback costs due to the selected optimal load recovery 652
schedule are again computed from two OPF runs in each time 653
step within the recovery window. Since load recovery increases 654
the amount of load, additional cost ΔLC is calculated as the 655
difference between costs with and without load recovery over 656
the load recovery period t_{REC} to t_{MAX} : 657

$$\Delta LC_i^s(t_{REC}) = LC_i^{s\ DR}(t_{REC}) - LC_i^{s\ NO-DR}(t_{REC}) \quad (22) \quad 658$$

$$C_{payback\ i}^s = \sum_{t=t_{REC}}^{t_{MAX}} \Delta LC_i^s(t) \quad (23) \quad 659$$

3) *Customer Profits*: The total customer profit $\pi_i^s(t_{RED})$ 660
needs to account for savings due to reduced load, costs due to 661
load recovery, as well as rewards for voluntary and involuntary 662
load shedding. This is summarised in the equation below: 663

$$664 \quad \pi_i^s(t_{RED}) = Savings_i^s - C_{payback\ i}^s + \sum_{t=t_{RED}}^{t_{REC}} IVLR_i^s(t) \quad 664$$

$$+ \sum_{t=t_{RED}}^{t_{REC}} VLR_i^s(t) \quad (24) \quad 665$$

Only load customer with a positive profit $\pi_i^s(t_{RED})$ evaluated 666
at time t_{REC} proceeds into the DR strategy. The analysis con- 667
tinues until the convergence criterion on expected energy not 668
served is met. After having completed the SMCS procedure, 669
the algorithm goes straight to the outputs module. 670

671 G. Outputs Module

The outputs module generates several results related to the 672
load reductions, nodal prices, generation outputs, reliability 673
and financial indicators. They are briefly discussed below. 674

675 1) *Optimal Load Reductions and Recoveries*: PDFs of vol-
 676 untary and involuntary load reductions by load types and/or
 677 nodes are calculated for each hour in the 24-hourly period.
 678 These can be directly converted into energy not served PDFs.
 679 The corresponding mean and percentile values show the
 680 ‘likely’ distributions in the next 24-hourly period. PDFs of
 681 daily totals are also computed. Besides, conditional PDFs of
 682 the load recovery initiation times given the load reduction at
 683 certain hour are also produced.

684 2) *Generation Outputs*: PDFs of generator hourly produc-
 685 tions and costs, as well as total daily costs are computed.

686 3) *Nodal Marginal Prices*: PDFs of nodal marginal prices
 687 are produced for each hour in the considered 24-hourly period.
 688 Their expectations can be used as an indicator what the prices
 689 for rewarding generation and charging load customers will be
 690 next day.

691 4) *Reliability Indices*: Reliability indices relating to energy
 692 not served as well as frequency of customer interruptions and
 693 duration of interruptions are computed. For example, expected
 694 energy not supplied (*EENS*), expected frequency of interrup-
 695 tions (*EFI*) and expected duration of interruptions (*EDI*) are
 696 calculated as:

$$\begin{aligned}
 697 \quad EENS &= \sum_{y=1}^Y \sum_{t=1}^T \sum_{i=1}^N \sum_{s=1}^{s_4} P c_i^s / Y, \\
 698 \quad EFI &= \sum_{y=1}^Y \sum_{t=1}^T \sum_{i=1}^N \sum_{s=1}^{s_4} \zeta_i^s / Y \\
 699 \quad EDI &= \sum_{y=1}^Y \sum_{t=1}^T \sum_{i=1}^N \sum_{s=1}^{s_4} \zeta_i^s \cdot D_i^s / Y. \quad (25)
 \end{aligned}$$

700 5) *Financial Indicators*: PDFs of load customer pay-
 701 ments (*LC*), voluntary (*VLR*) and involuntary load reduction
 702 rewards (*IVLR*) are computed by hours and for the considered
 703 day. The latter curves are then used to quantify the financial
 704 risk of implementing the proposed demand response schedul-
 705 ing. The concept of value-at-risk (*VaR*) [30] was applied
 706 to measure the potentially ‘low’ revenues or ‘excessive’
 707 payments.

708 Assuming network reward (*NR*) denotes any category of
 709 revenues, the corresponding cumulative distribution func-
 710 tion (CDF_{NR}) is used to calculate the network reward NR_X
 711 that exceeds the network reward at the confidence level α ,
 712 NR_α , with probability $1 - \alpha$. The value at risk is [31]:

$$713 \quad VaR_\alpha^{NR}(NR_X) = \inf\{NR_\alpha \in \mathbb{R} : CDF_{NR_X}(NR_\alpha) \geq \alpha\} \quad (26)$$

714 Similarly, the *CDF* of any network cost (*NC*) can be used
 715 to determine value-at-risk at confidence level α . In this case,
 716 network cost NC_X that does not exceed the network cost at
 717 probability $1 - \alpha$, $NC_{1-\alpha}$, is calculated as:

$$718 \quad VaR_{1-\alpha}^{NC}(NC_X) \\
 719 \quad = \sup\{NC_{1-\alpha} \in \mathbb{R} : CDF_{NC_X}(NC_{1-\alpha}) \leq 1 - \alpha\}. \quad (27)$$

720 IV. BULK ELECTRIC POWER SYSTEM

721 This section describes some practical aspects of the ampac-
 722 ity calculation of OHLs, modelling of wind farms, as well as
 723 the designed case studies.

TABLE I
 CONDUCTOR PROPERTIES MODELED IN IEEE-RTS NETWORK

NAME	<i>Rac</i> (Ω/Km)	<i>Configuration</i>	<i>S_{NORM}</i> (<i>MVA</i>)	<i>S_{EM-LONG}</i> (<i>MVA</i>)
Dove (138kV)	0.1003 @ 25°C 0.1270 @ 75°C	Single bundle	95 [60°C]	138 [75°C]
Hawk (230kV)	0.1154 @ 25°C 0.1225 @ 75°C	Twin bundle	308 [60°C]	365 [75°C]

724 A. Thermal Ratings of Overhead Lines

The IEEE-RTS 96 test system does not provide any OHL
 data required for the RTTR calculations. A simple ACSR tech-
 nology was assumed with conductor sizes that provide similar
 ratings to those in the IEEE-RTS 96 system with AAAC and
 ACSR conductors. Table I provides the information on the con-
 ductors used in the analysis. Under normal operation conductor
 temperature, T_c , is set to 60°C. A line is considered in emer-
 gency state when another transmission line connected at the
 same bus fails. The maximum conductor temperature in emer-
 gencies is set to 75°C based on avoidance of the conductor
 annealing [32].

736 B. Integration of Wind Farms

The power output of a wind turbine generator (WTG) is
 driven by the wind speed and the corresponding relationship is
 nonlinear. It can be described using the operational parameters
 of the WTG, such as cut-in, rated and cut out wind speeds.
 The hourly power output is obtained from the simulated hourly
 wind speed using the relations [33]:

$$\begin{aligned}
 743 \quad P(V_m) \\
 744 \quad = \begin{cases} 0, & 0 \leq V_m < V_{ci} \\ (A + B \times V_m + C \times V_m^2) \times P_r, & V_{ci} \leq V_m < V_r \\ P_r, & V_r \leq V_m < V_{co} \\ 0, & V_m \geq V_{co} \end{cases} \quad (28) \\
 745
 \end{aligned}$$

where P_r , V_{ci} , V_r , and V_{co} are, respectively, rated power out-
 put, cut-in wind speed, rated wind speed and cut-out wind
 speed of the WTG, whilst V_m is simulated wind speed at
 hour t . The power output constants A , B and C are determined
 by V_{ci} , V_r , and V_{co} , as shown in [33]. All WTG units used
 in this study are assumed to have cut-in, rated, and cut-out
 speeds of 14.4, 36, and 80km/h, respectively. The failure rates
 and average repair times are assumed to be two failures/year
 and 44 hours.

755 C. Case Study Description

OHL thermal ratings are modelled as STR or RTTR, as
 shown in Table II below. Three seasons (winter, summer and
 fall), denoted as $\lambda_s = 1, 2, 3$, are studied. The first day of
 the 50th peak week of the year is used for winter (hours:
 8425-8449); the 2nd day of the 22nd week of the year is
 used for summer (hours: 3721-3744) and the 2nd day of the
 32nd week is used for fall (hours: 5401-5424). Availability
 factor f_{RED}^s is a random number, whilst availability factor
 for load recovery f_{REC}^s varies in the specified range. Load

TABLE II
MODELING SCENARIOS OF DR METHODOLOGY

	S1	S2	S3	S4	S5	S6	S7	S8
p	STR	STR	STR	STR	RTTR	RTTR	STR	STR
λ_s	1,2,3	1	1,2,3	1	1	1	1	1
f_{RED}^s	0	1	1	1	0	1	0	1
f_{REC}^s	0	1	1	0-1.2	0	1	0	1
ϑ_{REC}	-	0	1	1	-	1	-	1
wg	0	0	0	0	0	0	1	1

recovery is based on either hourly emergency energy prices (i.e., $\vartheta_{REC} = 1$) or load profiles (i.e., $\vartheta_{REC} = 0$). The presence of wind generators is denoted by $wg=1$.

Eight scenarios are described in Table II. Scenario S1 is the base case, where the system is evaluated without DR scheduling and with standard thermal ratings for OHLs. Scenario S2 models load recovery by using the hourly load curve at each load point ($\vartheta_{REC} = 0$). Scenario S3 models all seasons and load recovery on the basis of expected marginal prices at each load point ($\vartheta_{REC} = 1$). Scenario S4 models time-varying load recovery profiles. Sensitivity studies are done here in order to assess the impact of different recovery sizes and profiles on DR performance. Factor f_{REC}^s is set from 0 to 1.2pu increasing in 0.2pu increments; the 1.2pu is taken as a high-risk scenario. Scenario S5 incorporates the RTTR of OHLs without DR operation, while Scenario S6 includes the DR scheduling. Finally, Scenario S7 incorporates wind farms without DR, while in Scenario S8 the benefits of demand response are evaluated incorporating wind generation ($wg=1$).

The original IEEE-RTS 96 was modified: all scenarios assume an increase in load by 1.2pu compared to the original load, as well as increase of 0.55pu and 0.6pu transmission capacity for the 138kV and 230kV levels, respectively, and 1.2pu in generation capacity. Next, the WTGs are connected at seven sites and it was assumed that they operate at power factor mode with power factor equal 35% [34]. Wind farms are designed to deliver 20% of the peak load [35], equivalent to 684MW on the studied power network. Geographically, 70% of the wind farms' maximum capacity is installed in the northern part of the network at buses 15, 17, 19, 20, 22, while in the southern part of the network, the remaining 30% of the wind capacity is installed to at buses 1, 2, 7, 8. The total wind farm capacity is 2394 MW obtained from a total number of 240 WTG, each representing a nominal capacity of 10MW. There is significant transmission utilization in this modified system as the bulk of the generating capacity is located mainly in the northern areas and considerable power is transferred from the north to the south aiming to represent the existing topology of the U.K. network. The analysis will study potential low wind output conditions in combination with unexpected network components failures.

V. CASE STUDY ANALYSIS

The IEEE-RTS 96 is composed of 38 lines circuits, 32 generating units and 17 load delivery points [36].

It is studied by using the algorithms developed in Matlab that make use of a modified version of Matpower and MIPS

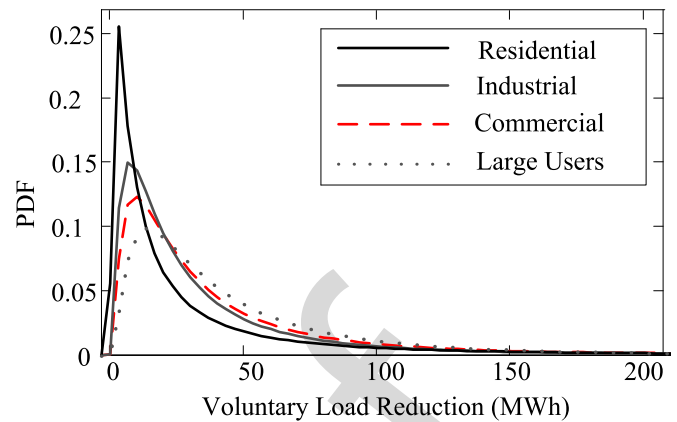


Fig. 3. Probability to respond to a DR signal for different customer types based on the voluntary load reduction amount at 17h00.

solver for the power flow calculations [37]. Essential study results on the eight scenarios related to the availability for load reduction, impact of nodal marginal prices, load recovery profile – availability, and impact of RTTR, DR and wind generation, are presented below.

A. Customer Availability for Load Reductions

In this section, the impact of the availability of customers responding to a DR call is examined. Uncertainty in load availability for each customer type is given by equation (18). In particular, domestic customers' load reduction takes values from the entire possible range, while for industrial and commercial loads it is within the assumed window, $win=0.8-1pu$. Scenario 3 (S3) is used to evaluate the impact of customers responding to a DR on the *EENS*, mean and *Var* values of voluntary (VLR) and involuntary load reductions (IVLR) – eqs. (12) and (13). For VLRs, Fig. 3 (generated over the entire MCS period) shows that the probability for residential loads to give 'small' response (up to 25 MWh) is much higher than to produce 'large' response (up to 50MWh).

However, industrial, commercial and large users are more likely to give 'larger' responses as they have bigger contracted amounts compared to residential users, and the uncertainty in response (if any) is much lower. For low load reductions, industrial loads have higher probability to respond than commercial and large users, while large users have the highest probability for larger amounts of load reductions; they are followed by commercial and industrial users.

The PDFs for voluntary (VL) and involuntary (IVL) load reductions for different hours in a day are illustrated in Fig. 4 and compared with the PDF of IVL without DR ($IVL^{NO\ DR}$). The results show that the probability of having IVL is reduced when doing DR (IVL^{DR}) with higher amounts (right side of x-axis), while the probability is much higher for low amounts of IVL. This clearly shows the effectiveness of voluntary DR on the *EENS*. In particular, the mean value of IVL^{DR} at 17h00 is around 60% less than the mean value of $IVL^{NO\ DR}$. A similar conclusion applies to all hours; for example, the mean of IVL^{DR} at 21h00 and 22h00 is, respectively, 61% and 60% lower when applying the voluntary DR. Applying

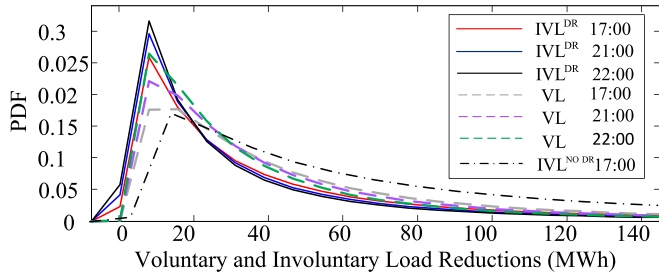


Fig. 4. Probability of voluntary and involuntary load reductions under DR for different hours in a day.

TABLE III
VAR VALUES OF CUSTOMERS COSTS AND REWARDS (k£)

Critical buses	B6		B8		B14	
	S1	S3	S1	S3	S1	S3
VaR _{50%} ^{LC}	31.43	19.59	55.13	22.91	57.55	41.72
VaR _{90%} ^{LC}	55.64	52.81	75.11	61.24	95.39	89.08
VaR _{50%} ^{VLR}	-	1.3	-	1.8	-	1.5
VaR _{90%} ^{VLR}	-	5.6	-	2.5	-	2.8
VaR _{50%} ^{IVLR}	600	240	578	320	480	252
VaR _{90%} ^{IVLR}	1344	420	1260	604	1284	546

voluntary load reduction (VL) helps eliminate the need for involuntary one (IVL^{NO DR}), particularly when larger VL amounts are used. This is further highlighted when converting VL and IVL into the EENS index (see Table IV in Section V-B).

Table III shows the mean (VaR_{50%}) and the 90% confidence VaR (VaR_{90%}) for the costs for demand (LC), for VLR and IVLR revenues for the most critical load points (B6, B8 and B14) under scenarios S1 and S3. Both the VaR_{50%}^{LC} and VaR_{90%}^{LC} are much lower under S3 for all load points, since under DR, demand is recovered under cheaper nodal marginal prices.

In addition, VaR_{90%}^{VLR} is much larger than VaR_{50%}^{VLR} since marginal nodal prices are significantly higher under emergency conditions. Furthermore, the VaR_{50%}^{IVLR} is much lower under S3 than under S1, where it decreases by 60% for B6, 44% for B8 and 47% for B14. This also shows that voluntary DR significantly decreases the need for IVL (an average VOLL value was assumed for all customer types).

B. Impact of Nodal Prices on Reliability Analysis

Most DR studies would recover reduced load during load troughs and/or system normal if only network adequacy were looked at.

However, we have used the approach to investigate impact of hourly nodal prices on load recovery and customers' well-being. Fig. 5 shows an example of the nodal marginal price and the demand variation in time for the most frequently interrupted bus in the network (B6) under both intact and emergency conditions.

When no failures occur, load can be recovered almost at any time since intact prices do not change significantly with

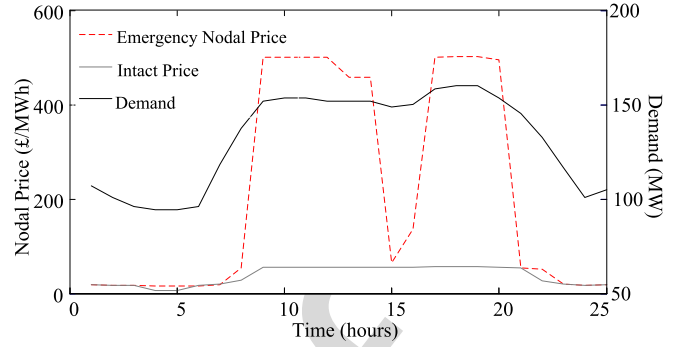


Fig. 5. Hourly marginal prices and demand curve under emergency for Bus 6.

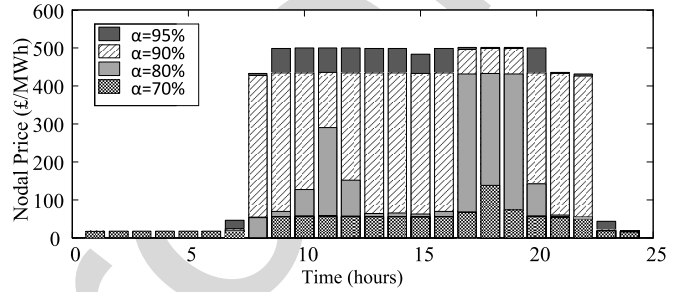


Fig. 6. Emergency marginal price for different confidence levels.

respect to load. However, nodal prices under emergency conditions may vary considerably. For instance, a significant shape difference between intact and emergency nodal prices is shown at 15h00. Our analysis has proven that the magnitude of the emergency nodal price can be almost 5 times higher than the intact one. Thus, scheduling of 'optimal' load recoveries based on marginal nodal prices has proven effective in providing system security and customer benefits. Furthermore, comparative studies were conducted to quantify the improvements from implementing load recovery under nodal marginal prices rather than under load profile only.

The hourly nodal price at bus B6 for different confidence levels is given in Fig. 6. In the event of an emergency at B6, TSOs may be provided with the illustrated confidence level dependent prices to decide which load recovery hour would be the most appropriate to restore load. For example, the TSO can know that if a violation occurs at 11h00, the load can be recovered between 13h00 and 16h00, since there is an 80% probability that the price will be between zero and 90£/MWh and a 90% probability that the price will be between zero and 420£/MWh. In this paper, a conservative confidence level of $\alpha = 95%$ was selected. This gives flexibility to TSOs to apply operational decisions so they can guarantee making a profit for the demand customers for almost all nodal prices in the feasible range, since the load recovery will be at either the emergency nodal prices or (lower) intact prices.

The results presented in Table IV show that DR strategy under scenario S3 improves the reliability of the network in terms of EENS by 66% in winter ($\lambda_s = 1$) compared with S1, allowing for almost a 5% decrease in EENS compared to S2. The S3 strategy also substantially improves reliability indices

TABLE IV
RELIABILITY INDICES FOR SCENARIOS 1, 2 AND 3

S	EENS(MWh/day)			EDI(*10 ⁻³ h/day)			EFI(int/day)		
	1	2	3	1	2	3	1	2	3
λ_s	1	2	3	1	2	3	1	2	3
S1	577	160.5	36.4	23.9	9.7	0.99	0.039	0.0156	0.00234
S2	206	59.2	12.9	23.2	9.2	0.57	0.0385	0.0154	0.00231
S3	196	42.8	4.8	23.3	8.5	0.35	0.0383	0.01532	0.00229

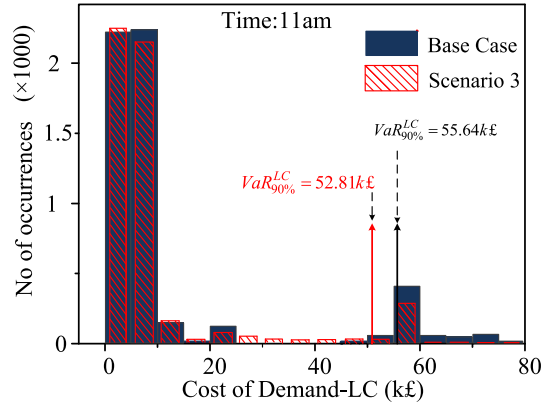


Fig. 7. Distribution of demand costs for load at Bus 6.

TABLE V
RELIABILITY INDICES FOR SCENARIO 4

f_{REC} (pu)	1.2	1	0.8	0.6	0.4	0.2
EENS(MWh/day)	205.8	196	192.34	191.13	191.08	188.12
EDI(h/day)	0.2334	0.2331	0.2330	0.229	0.227	0.227
EFI(int/day)	0.0386	0.0383	0.0383	0.038	0.038	0.0378

for summer ($\lambda_s = 2$) and fall ($\lambda_s = 3$), which demonstrates the effectiveness of the algorithm throughout the year.

In order to show the necessity to quantify the economic risk of DR operation, results for the base case S1 are compared to scenario S3 to investigate the VaR of the load cost (LC). Fig. 7 illustrates frequency of occurrence of various load costs seen at the most critical bus, B6, with and without DR. In particular, it is shown that there is a high variation in nodal costs at 11h00, resulting from outages of lines 12 and 13 that connect B6 with cheaper generators. Consequently, $VaR_{90\%}^{LC}$ is 55.64k£ under the base case, whereas it is only 52.81k£ under S3, which shows that DR can help reduce nodal costs by 5% (2.83k£). Clearly, both reliability and financial indices can be improved using nodal energy prices (S3) rather than the load profile only (S2).

C. Impact of Customer Availability to Recover the Load

The load recovery of a DR customer can be of different size compared to the corresponding load reduction. As a result, this can affect both the network performance and customer profits, as exemplified by scenario S4.

Assuming load recovery size is specified by availability factor f_{REC}^s , Table V shows an increase of around 5% in EENS for $f_{REC}^s = 1.2pu$ compared to $f_{REC}^s = 1pu$. When load recovery sizes are lower than 100%, network reliability is improved compared to $f_{REC} = 1pu$. This is due to the higher probability of implementing voluntary DR since less load recoveries

TABLE VI
DIFFERENCE IN MEAN AND VAR FOR LC (£) AND PROFITS (£/KWH) S4 VS. S3

S5	S4-S3 Values			
	$VaR_{50\%}^{LC}$	$VaR_{90\%}^{LC}$	$VaR_{50\%}^{\pi}$	$VaR_{90\%}^{\pi}$
$f_{REC}^s = 1.2$	+912	+1932	+0.05	+0.2
$f_{REC}^s = 0.8$	-89	+775	+5.3	+8.1
$f_{REC}^s = 0.6$	-101	-198	+6.3	+9.5
$f_{REC}^s = 0.4$	-257	-2102	+8.8	+9.5
$f_{REC}^s = 0.2$	-463	-2124	+10.2	+12.8

TABLE VII
IEEE RTS NETWORK EVALUATION WITH RTTR & DR

Reliability indices	Scenarios	S3	S5	S6
	EENS(MWh/day)		196	475
EFI (int/day)		0.0383	0.0381	0.0379
EDI*10 ⁻² (h/day)		23.31	23.34	23.18
Financial indices (k£)	$VaR_{50\%}^{LC}$	135.9	134.9	131.3
	$VaR_{90\%}^{LC}$	142.7	136.1	134.8
	$VaR_{50\%}^{VLR}$	1.6	-	1.2
	$VaR_{50\%}^{IVLR}$	2352	-	2196

are required. There is also a substantial decrease in reliability indices EDI and EFI.

Differences in the mean ($VaR_{50\%}$) and $VaR_{90\%}$ values for demand costs (LC) and customer profits (π) between scenarios S4 and S3 are shown in Table VI for different load recovery sizes f_{REC}^s . This table gives the cost and revenue differences following various load payback sizes compared to applying DR with a load payback of 100% for a winter day-ahead operation. For instance, when S4 is modeled with $f_{REC} = 1.2pu$, the $VaR_{50\%}^{LC}$ is 912£ higher than under scenario S3. This is because as load recovery gets larger, the operating conditions become more difficult and the marginal prices increase, implying higher costs for demand. For low load recovery sizes, however, very high profits can be incurred (over 2,100£) as the demand cost VaR shows the largest decrease, thus suggesting a much lower probability of high LC.

D. Impact of RTTR and DR on Network Reliability and Customer Costs & Revenues

In scenario S5 only RTTR is used, whilst scenario S6 makes use of DR in conjunction with RTTR. Table VII shows that the more reliable and cheapest scenario is S6.

The use of RTTR and DR under S6 results in, respectively, 61% and 6.6% reduction in EENS compared with DR alone (S3) and with S5. Indices EFI and EDI are also improved. When RTTR is considered alone (S5), the greater utilization of the three most critical lines improves network performance by 18% compared to S1. Besides, the load cost index for S3 $VaR_{50\%}^{LC}$ is slightly higher than $VaR_{50\%}^{LC}$ for S5. This is because RTTR allows greater generation from cheaper units.

In terms of VLR and IVLR, both average values are lower under S6.

TABLE VIII
IEEE RTS NETWORK EVALUATION OF WIND FARMS & DR

Scenarios		S3	S7	S8
Reliability indices	EENS(MWh/day)	196	496	189
	EFI (int/day)	0.0383	0.0388	0.0383
	EDI*10 ⁻² (h/day)	23.31	23.8	23.19
Financial indices (k£)	VaR _{50%} ^{LC}	135.9	135.3	129.3
	VaR _{90%} ^{LC}	142.7	141.9	136.8
	VaR _{50%} ^{VLR}	1.6	-	1.05
	VaR _{50%} ^{IVLR}	2352	-	2268

We can note that DR provides the greatest benefits since all indices are drastically improved with DR, whilst benefits are only slightly higher under RTTR.

E. Impact of Wind Farms and DR on Network Reliability and Customer Costs & Revenues

In scenario S7, only wind farms are used, whilst scenario S8 uses DR in conjunction with wind farms. Table VIII shows that the more reliable and less expensive scenario is S8; the wind farms contribute to improving network reliability by 4% in EENS compared with S3 alone. Besides, a considerable reduction in EDI is achieved, whilst frequency of interruptions, EFI, remains the same as under S3. If compared with S1, wind farms alone (S7) improve network performance by 14% due to wind farms' network reinforcements. Also, VaR_{50%}^{LC} for S3 is slightly higher than VaR_{50%}^{LC} for S7 as wind farms are considered to have near-zero marginal costs. When wind farms are used in conjunction with DR (S8), this has the best effect on network performance and customer costs & revenues. This is because DR implementation helps when wind output is low and network components fail. Next, when wind output is high, spillage can occur as there is not enough capacity on the network to transfer the total amount of wind, thus leading to congestion when using STR for OHL operation. This can result in a small reduction of EENS.

VI. CONCLUSION

A probabilistic methodology for optimal scheduling of load reductions/recoveries in a day-ahead planning of transmission networks is proposed in the paper. The methodology recognizes several types of uncertainties, and finds optimal demand response scheduling using the network security and customer economics criteria. Impacts of wind generation and real-time thermal ratings of overhead lines are also studied.

The developed case studies have demonstrated that the value of optimal demand scheduling combined with real-time thermal ratings can be significant when using nodal marginal prices compared to using the hourly loads only. In particular, both reliability and financial metrics can be improved by a factor of around 66% for expected energy not served and around 5% for value at risk for costs of demand. Improvements in other reliability indicators and expected generation costs were also observed. Nonetheless, selection of the reliability indicator to base the operational decisions on demand scheduling can

be of highest importance; having multiple indices can therefore help system operators to make more informed decisions on 'best' demand response practice. As a final comment, the consistent use of a probabilistic approach to model various network uncertainties and variability of nodal marginal prices provides a superior analysis compared to traditional analytical techniques.

The future work considers inclusion of optimal energy storage scheduling to increase system reliability. Combined impact of energy storage, demand response and wind generation will be studied in greater detail.

REFERENCES

- P. Denholm and M. Hand, "Grid flexibility and storage required to achieve very high penetration of variable renewable electricity," *Energy Pol.*, vol. 39, no. 3, pp. 1817–1830, 2011.
- D. T. Nguyen, M. Negnevitsky, and M. de Groot, "Pool-based demand response exchange—Concept and modeling," *IEEE Trans. Power Syst.*, vol. 26, no. 3, pp. 1677–1685, Aug. 2011.
- A. S. Deese, E. Stein, B. Carrigan, and E. Klein, "Automation of residential load in power distribution systems with focus on demand response," *IET Gener. Transm. Distrib.*, vol. 7, no. 4, pp. 357–365, Apr. 2013.
- P. Wang, Y. Ding, and Y. Xiao, "Technique to evaluate nodal reliability indices and nodal prices of restructured power systems," *IEE Proc. Gener. Transm. Distrib.*, vol. 152, no. 3, pp. 390–396, May 2005.
- M. Fotuhi-Firuzabad and R. Billinton, "Impact of load management on composite system reliability evaluation short-term operating benefits," *IEEE Trans. Power Syst.*, vol. 15, no. 2, pp. 858–864, May 2000.
- E. Karangelos and F. Bouffard, "Towards full integration of demand-side resources in joint forward energy/reserve electricity markets," *IEEE Trans. Power Syst.*, vol. 27, no. 1, pp. 280–289, Feb. 2012.
- D. T. Nguyen, M. Negnevitsky, and M. de Groot, "Modeling load recovery impact for demand response applications," *IEEE Trans. Power Syst.*, vol. 28, no. 2, pp. 1216–1225, May 2013.
- N. Ruiz, I. Cobelo, and J. Oyarzabal, "A direct load control model for virtual power plant management," *IEEE Trans. Power Syst.*, vol. 24, no. 2, pp. 959–966, May 2009.
- A. Molina-Garcia, F. Bouffard, and D. S. Kirschen, "Decentralized demand-side contribution to primary frequency control," *IEEE Trans. Power Syst.*, vol. 26, no. 1, pp. 411–419, Feb. 2011.
- C. L. Su and D. Kirschen, "Quantifying the effect of demand response on electricity markets," *IEEE Trans. Power Syst.*, vol. 24, no. 3, pp. 1199–1207, Aug. 2009.
- R. Billinton and W. Li, *Reliability Assessment of Electrical Power Systems Using Monte Carlo Methods*. London, U.K.: Plenum, 1994.
- J. Schachter and P. Mancarella, "A short-term load forecasting model for demand response applications," in *Proc. IEEE 11th Int. Conf. Eur. Energy Market (EEM)*, Krakow, Poland, 2014, pp. 1–5.
- "The value of lost load (VoLL) for electricity in Great Britain: Final report for OFGEM and DECC," London Econ., London, U.K., Tech. Rep., 2013.
- Current Rating Guide for High Voltage Overhead Lines Operating in the UK Distribution System*, document ER. P27, Energy Netw. Assoc., London, U.K., 1986.
- IEEE Standard for Calculating the Current-Temperature of Bare Overhead Conductors*, IEEE Standard 738-2006, 2007, pp. 1–59.
- [Online]. Available: <http://badc.nerc.ac.uk/data/ukmo-midas/WPS.html>
- J. M. Arroyo and F. D. Galiana, "Energy and reserve pricing in security and network-constrained electricity markets," *IEEE Trans. Power Syst.*, vol. 20, no. 2, pp. 634–643, May 2005.
- M. S. Bazaraa, J. J. Jarvis, and H. D. Sherali, *Linear Programming and Network Flows*, 4th ed. Hoboken, NJ, USA: Wiley, 2010.
- I. J. Perez-Arriaga and C. Meseguer, "Wholesale marginal prices in competitive generation markets," *IEEE Trans. Power Syst.*, vol. 12, no. 2, pp. 710–717, May 1997.
- K. Singh, N. P. Padhy, and J. Sharma, "Influence of price responsive demand shifting bidding on congestion and LMP in pool-based day-ahead electricity markets," *IEEE Trans. Power Syst.*, vol. 26, no. 2, pp. 886–896, May 2011.
- X. Cheng and T. J. Overbye, "An energy reference bus independent LMP decomposition algorithm," *IEEE Trans. Power Syst.*, vol. 21, no. 3, pp. 1041–1049, Aug. 2006.

- 1081 [22] S. Wong and J. D. Fuller, "Pricing energy and reserves using stochastic
1082 optimization in an alternative electricity market," *IEEE Trans. Power*
1083 *Syst.*, vol. 22, no. 2, pp. 631–638, May 2007.
- 1084 [23] D. S. Kirschen, K. R. W. Bell, D. P. Nedic, D. Jayaweera, and
1085 R. N. Allan, "Computing the value of security," *IEE Proc. Gener.*
1086 *Transm. Distrib.*, vol. 150, no. 6, pp. 673–678, Nov. 2003.
- 1087 [24] G. Dorini, P. Pinson, and H. Madsen, "Chance-constrained optimization
1088 of demand response to price signals," *IEEE Trans. Smart Grid*, vol. 4,
1089 no. 4, pp. 2072–2080, Dec. 2013.
- 1090 [25] C. Chen, J. Wang, and S. Kishore, "A distributed direct load control
1091 approach for large-scale residential demand response," *IEEE Trans.*
1092 *Power Syst.*, vol. 29, no. 5, pp. 2219–2228, Sep. 2014.
- 1093 [26] A. Abdollahi, M. P. Moghaddam, M. Rashidinejad, and
1094 M. K. Sheikh-El-Eslami, "Investigation of economic and environmental-
1095 driven demand response measures incorporating UC," *IEEE Trans.*
1096 *Smart Grid*, vol. 3, no. 1, pp. 12–25, Mar. 2012.
- 1097 [27] M. H. Albadi and E. F. El-Saadany, "A summary of demand response
1098 in electricity markets," *Elect. Power Syst. Res.*, vol. 78, no. 11,
1099 pp. 1989–1996, 2008.
- 1100 [28] E. Agneholm and J. Daalder, "Load recovery in different industries fol-
1101 lowing an outage," *IEE Proc. Gener. Transm. Distrib.*, vol. 149, no. 1,
1102 pp. 76–82, Jan. 2002.
- 1103 [29] G. Strbac, E. D. Farmer, and B. J. Cory, "Framework for the incorpo-
1104 ration of demand-side in a competitive electricity market," *IEE Proc.*
1105 *Gener. Transm. Distrib.*, vol. 143, no. 3, pp. 232–237, May 1996.
- 1106 [30] "National grid EMR analytical report," Nat. Grid, Warwick, U.K., Tech.
1107 Rep., 2013.
- 1108 [31] A. Shapiro and S. Basak, "Value-at-risk based risk management: Optimal
1109 policies and asset prices," *Rev. Financ. Stud.*, vol. 14, no. 2, pp. 371–405,
1110 2001.
- 1111 [32] K. Kopsidas, S. M. Rowland, and B. Boumeceid, "A holistic method for
1112 conductor ampacity and sag computation on an OHL structure," *IEEE*
1113 *Trans. Power Del.*, vol. 27, no. 3, pp. 1047–1054, Jul. 2012.
- 1114 [33] P. Giorsetto and K. F. Utsurogi, "Development of a new procedure for
1115 reliability modeling of wind turbine generators," *IEEE Trans. Power*
1116 *App. Syst.*, vol. PAS-102, no. 1, pp. 134–143, Jan. 1983.
- 1117 [34] *Renewable Sources of Energy*, Dept. Energy Climate Change, Dig. U.K.
1118 Energy Stat., London, U.K., 2014, pp. 157–193.
- 1119 [35] K. Soren, M. Poul-Eric, and A. Shimon, *Wind Energy Implications of*
1120 *Large-Scale Deployment on the GB Electricity System*, Roy. Acad. Eng.,
1121 London, U.K., 2014, p. 72.
- 1122 [36] C. Fong *et al.*, "The IEEE reliability test system-1996. A report prepared
1123 by the reliability test system task force of the application of probabili-
1124 ty methods subcommittee," *IEEE Trans. Power Syst.*, vol. 14, no. 3,
1125 pp. 1010–1020, Aug. 1999.
- 1126 [37] R. D. Zimmerman, E. M.-S. Carlos, and D. Gan, *MATPOWER:*
1127 *A MATLAB Power System Simulation Package, Version 3.1b2, User's*
1128 *Manual*, Power Systems Eng. Res. Center, New York, NY, USA, 2011.



Manchester, with main research interests on plant modeling and reliability and adequacy.

1141



Alexandra Kapetanaki (S'12) received the M.Eng. degree in electrical engineering and computer science from the National Technical University of Athens, Greece, in 2011. She is currently pursuing the Ph.D. degree with the Electrical Energy and Power Systems Group.

Her current research interests include optimization of power system operation, stochastic modelling, risk management, and electricity markets.

1150



Victor Levi (S'89–M'91–SM'13) received the M.Sc. and Ph.D. degrees in electrical engineering from the University of Belgrade, Belgrade, Yugoslavia, in 1986 and 1991, respectively.

From 1982 to 2001, he was with the University of Novi Sad, Novi Sad, Yugoslavia, where he became a Full Professor in 2001. He was with the University of Manchester, Manchester, U.K., from 2001 to 2003, and then with United Utilities and Electricity North West from 2003 to 2013. In 2013, he rejoined the University of Manchester.

1161

AUTHOR QUERIES

AUTHOR PLEASE ANSWER ALL QUERIES

PLEASE NOTE: We cannot accept new source files as corrections for your paper. If possible, please annotate the PDF proof we have sent you with your corrections and upload it via the Author Gateway. Alternatively, you may send us your corrections in list format. You may also upload revised graphics via the Author Gateway.

AQ1: Please provide the author name, department name, and technical report number for References [13] and [30].

AQ2: Please verify and confirm the edits made to References [14], [34], [36], and [37] are correct as set.

AQ3: Please provide the title and accessed date for Reference [16].

IEEE PROOF

Optimal Demand Response Scheduling With Real-Time Thermal Ratings of Overhead Lines for Improved Network Reliability

Konstantinos Kopsidas, *Member, IEEE*, Alexandra Kapetanaki, *Student Member, IEEE*, and Victor Levi, *Senior Member, IEEE*

Abstract—This paper proposes a probabilistic framework for optimal demand response scheduling in the day-ahead planning of transmission networks. Optimal load reduction plans are determined from network security requirements, physical characteristics of various customer types, and by recognizing two types of reductions, voluntary and involuntary. Ranking of both load reduction categories is based on their values and expected outage durations, while sizing takes into account the inherent probabilistic components. The optimal schedule of load recovery is then found by optimizing the customers' position in the joint energy and reserve market, while considering several operational and demand response constraints. The developed methodology is incorporated in the sequential Monte Carlo simulation procedure and tested on several IEEE networks. Here, the overhead lines are modeled with the aid of either static-seasonal or real-time thermal ratings. Wind generating units are also connected to the network in order to model wind uncertainty. The results show that the proposed demand response scheduling improves both reliability and economic indices, particularly when emergency energy prices drive the load recovery.

Index Terms—Optimal demand response, reliability, sequential Monte-Carlo, real time thermal rating, risk.

NOMENCLATURE

The symbols used throughout this paper are defined below.

Indices

j	Index of generating units running from 1 to J
i	Index of load points running from 1 to N
s	Index of load types running from 1 to s_4
t	Index of hours running from 1 to T
y	Index of simulation days running from 1 to Y.

Parameters

$VOLL_i^s$	Value of lost load at load point i and load type s
------------	--

Manuscript received April 26, 2015; revised August 22, 2015 and November 27, 2015; accepted March 6, 2016. This work was supported by the Engineering and Physical Sciences Research Council within the HubNet Project under Grant EP/I013636/1. Paper no. TSG-00463-2015.

The authors are with the School of Electrical and Electronic Engineering, Electrical Energy and Power Systems Group, University of Manchester, Manchester M13 9PL, U.K. (email: k.kopsidas@manchester.ac.uk; alexandra.kapetanaki@manchester.ac.uk; victor.levi@manchester.ac.uk).

Color versions of one or more of the figures in this paper are available online at <http://ieeexplore.ieee.org>.

Digital Object Identifier 10.1109/TSG.2016.2542922

$\hat{B}EDI_i$	Normalized value of expected duration interruption index in the base case	34
D_i^s BASE	Duration of interruption of load type s at load point i under the base case	35
P_g^{\max}	Maximum power output of a generation unit	36
P_g^{\min}	Minimum power output of a generation unit	37
P_d^{\max}	Maximum forecast load	38
$VL_i^{s,\max}$	Upper limit of the voluntary load reduction for customer type s	39
$IVL_i^{s,\max}$	Upper limit of the involuntary load reduction for customer type s	40
B	System matrix including potential contingencies	41
win	Per unit window for load reduction sampling	42
rs	Random number between $\{0,1\}$	43
t_{MAX}	Maximum hour limit of load recovery	44
f_{REC}^s	Customer's availability to recover the load	45
V_{ci}	Cut in wind speed	46
V_r	Rated wind speed	47
V_{co}	Cut out wind speed	48
P_r	Rated power output of wind turbine	49
$T_c(t)$	Conductor temperature at hour t	50
$R(t)$	AC conductor resistance at operating temperature T_c at hour t	51
$P_c(t)$	Convection heat loss at hour t	52
$P_r(t)$	Radiated heat loss at hour t	53
$P_s(t)$	Solar heat gain at hour t	54
$I(t)$	Conductor current at hour t	55
$V_m(t)$	Wind speed at hour t	56
$K_{angle}(t)$	Wind direction at hour t	57
$T_a(t)$	Ambient temperature at hour t .	58

Variables

$P_{g_j}(t)$	Active Power output of generation unit j at hour t	59
θ	Phase angles of nodal voltages	60
$\mu_i(t)$	Nodal marginal price of load point i at hour t	61
$\gamma_i^s(t)$	Slope coefficient for load recovery at node i , type s , hour t	62
P_f^{\max}	Overhead line real-time thermal rating	63
$P_{di}(t)$	Power supplied to load point i at hour t	64
$\sigma_i^s(t)$	Marginal offer value for voluntary load reduction, load type s at load point i at hour t	65

76	$VL_i^s(t)$	Amount of voluntary load reduction of load type s at load point i at hour t
77		
78	$IVL_i^s(t)$	Amount of involuntary load reduction of load type s at load point i at hour t
79		
80	$D_i^s(t)$	Duration of interruption of load type s at load point i at hour t
81		
82	$Pc_i^s(t)$	Total load shedding of load type s at load point i at hour t
83		
84	$f_{RED}^s(t)$	Load type s availability to respond to a demand response call at hour t
85		
86	$CVL_i^s(t)$	Contracted voluntary load reduction of load type s at load point i at hour t .
87		

88 Functions

89	$GR_j(\cdot)$	Revenue of generator j
90	$LC_i(\cdot)$	Cost of delivered demand at node i
91	$VLR_i(\cdot)$	Revenue for voluntary load type s reduction at node i
92		
93	$IVLR_i(\cdot)$	Revenue for involuntary load type s reduction at node i
94		
95	$\hat{R}_i^s(\cdot)$	Ranking order for load type s at node i
96	$[\Lambda^-]_i^s(\cdot)$	Size of load reduction for load point i type s
97	$[\Lambda^+]_i^s(\cdot)$	Size of load recovery for load point i type s
98	$Savings_i^s(\cdot)$	Customer savings for load point i type s in the event that demand response materializes
99		
100	$C_{payback}^s i(\cdot)$	Payback cost due to load recovery at node i type s
101		
102	$\pi_i^s(\cdot)$	Profit of load customer at load point i type s
103	$VaR_\alpha^{NR}(\cdot)$	Value at risk for network rewards at confidence level α
104		
105	$VaR_{1-\alpha}^{NC}$	Value at risk for network costs at confidence level $1-\alpha$
106		
107	$P(\cdot)$	Wind turbine power output for wind speed V_m .

108 I. INTRODUCTION

109 **T**HE EVER increasing integration of intermittent renewable energy into the electricity network, combined with
 110 a constantly growing demand, is likely to cause much greater
 111 stress on existing networks increasing the probability of
 112 severe contingencies [1]. To avoid this, several preventive and
 113 corrective actions, including demand response (DR), spinning
 114 reserve scheduling, application of real-time thermal ratings
 115 (RTTR) and energy storage scheduling, can be deployed
 116 to relieve stress in particular areas of the network.

117 DR strategies currently under investigation consider distribution level [2], [3], but their potential in transmission
 118 networks is often overlooked. Research related to the impact
 119 of DR on network reliability is very limited [4]–[6]. The
 120 model proposed in [5] evaluates short term operational benefits
 121 in terms of generation and interrupted energy costs from
 122 interruptible loads by using the contingency enumeration
 123 technique; however, it does not fully address the customer
 124 perspective because there is no modelling of load recovery and
 125 associated costs, characteristics of different load and DR types
 126 and probabilistic nature of available interruptible demand.
 127 Even if a probabilistic approach is used to assess the DR
 128 contribution [6], only single contingencies are analysed.

Physical characteristics of different types of load customers
 need to be adequately represented in the studies. Domestic
 and small commercial loads are analysed in [7]–[9] but fail to
 assess how critical each customer type is for a network's load
 point in terms of interruptions. Next, examining different sizes
 and shapes of both load reduction and recovery is essential for
 a complete and accurate network assessment; however, load
 recovery is usually ignored in the studies [4]. Load reduction
 and recovery can be based on electricity market prices in order
 to eliminate price spikes during peak hours [4], [10]. However,
 these studies often ignore operational and security constraints
 of the transmission networks and are run for intact networks
 only. Enumeration techniques, as opposed to Monte Carlo simulation,
 are often used to calculate the DR contribution, and thus fail to
 include the whole set of contingencies and a number of uncertainties
 a network might experience [11]. Finally, instead of applying DR
 every time a contingency occurs, DR should only be used when the
 reliability is improved and when savings are higher than the expected
 payback costs.

This paper proposes a probabilistic approach for optimal demand
 response scheduling in the day-ahead planning of transmission
 networks. Uncertainties related to forecast load, network component
 availability, available amount of demand response and wind speeds
 are incorporated into the sequential Monte Carlo simulation
 framework. Synchronous and wind generating units, as well as
 four types of load customers (large, industrial, commercial and
 residential) are modelled. Optimal nodal load reductions are
 calculated using the optimum power flow model, and are then
 disaggregated into voluntary and involuntary components. Recognizing
 that directly-controlled loads can certainly be shed and indirectly-
 controlled contain a probabilistic component, optimal amounts of
 voluntary and involuntary nodal reductions are determined. Different
 load recovery profiles for customer types are considered next within
 'payback periods' and they are initiated when the load customer's
 revenue is highest. Here, delivered load is priced at nodal marginal
 price, voluntary load reduction at marginal offer price and involuntary
 load reduction at damage cost. The whole analysis is implemented
 from the load customer's perspective to maximise their revenues,
 whilst the load recoveries are controlled by the transmission system
 operator (TSO); they may represent either physical paybacks from
 specific appliances or controlled paybacks whereby the TSO
 schedules its customer loads so as to have the desired shape. The
 benefits of optimal DR strategies are evaluated in combination with
 real-time thermal ratings of overhead lines to reveal the true
 potential of the DR. The outputs of the model also include financial
 risk quantifiers that the revenues are below, or costs are above a
 threshold.

180 II. OVERVIEW OF THE METHODOLOGY

Optimal DR scheduling is determined using the sequential Monte Carlo
 probabilistic approach. The main features of the proposed DR modeling
 framework are: a) Load reduction scheduling driven by network security;
 b) Optimal scheduling of load recovery using economic criteria;
 c) Modelling of real-time thermal ratings of overhead lines;

187 and d) Modelling of renewable energy sources, such as wind
188 generation.

189 The overall methodology is realized within two indepen-
190 dent sequential Monte Carlo simulation (SMCS) procedures.
191 The first SMCS is the initialization module, which is used to
192 calculate several components required by the second SMCS
193 that determines optimal day-ahead operation of the power sys-
194 tem. The main building blocks of the first SMCS procedure
195 are: a) Calculation of reliability indices needed for ranking
196 of load types for demand reduction; b) Calculation of real-
197 time thermal ratings of overhead lines; and c) Determination
198 of nodal marginal prices and several economic indicators used
199 for finding the optimal schedule of load recoveries.

200 The second SMCS consists of four modules: a) Demand
201 reduction scale module; b) Load recovery scale module;
202 c) Demand reduction and load recovery (DRLR) control mod-
203 ule, and d) The outputs module. The first module contains
204 ranking of different load types for demand reduction, calcu-
205 lation of required amounts of voluntary and involuntary DR,
206 as well as the customer revenues. The load recovery scale
207 module considers load recovery profiles and sizes, and deter-
208 mines a matrix with the most appropriate schedule hours for
209 load recovery. The DRLR-control module contains logics for
210 initiation of load reductions and load recoveries, whilst the
211 outputs module includes optimal load reduction and recovery
212 schedules, as well as reliability and financial indicators.

213 III. METHODOLOGY

214 The proposed demand scheduling methodology is aimed
215 at determining the optimal demand response plan for the
216 next day, when the committed generation units, status of net-
217 work switching devices and forecast loads are well defined.
218 However, several uncertainties in the day-ahead operation are
219 still present, so that the overall problem is formulated as
220 a probabilistic model and solved with the SMCS. The pro-
221 posed DR methodology is applied for post contingency states;
222 however it is general enough to also consider pre-contingency
223 events. The main building blocks are briefly presented below.

224 A. Sequential Monte Carlo Simulation

225 Sequential Monte Carlo simulation performs analysis of
226 time intervals in chronological order whilst taking into account
227 various uncertainties [11]. It can model the chronological
228 phenomena, such as load reduction and recovery, real-time
229 thermal ratings and wind generations. Following uncertainties
230 were assumed for a day-ahead operation of the transmission
231 network:

- 232 • Load varies in a window around the forecast hourly loads.
233 The uncertainty window is defined by the MAPE of the
234 short-term forecast by hourly intervals obtained using the
235 neural network approach [12].
- 236 • Availability of all generation and network units was mod-
237 elled with the aid of two-state Markovian model with
238 exponentially distributed up and down times [11].
- 239 • Wind speed hourly predictions and a window around the
240 predicted values are applied within the random sampling.

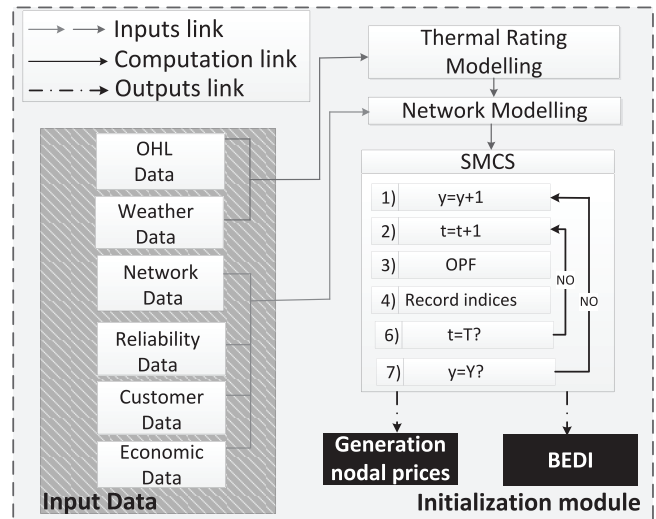


Fig. 1. Computations within the initialization module.

An alternative approach is to use wind speed probability
distribution functions (PDFs) by hourly periods.

- Amount of voluntary load reduction that varies by cus-
tomer and DR type. For example, DR from residential
customers responding to price signals is highly uncertain,
whilst DR from incentive-based contracted commercial
customers has much less uncertainty – see Section III-D.

One SMCS period is equal to 24 hours and simulations are
repeated until convergence is obtained. Any failure that goes
over the planning horizon (i.e., 24:00) was considered in the
'next day' simulation. The same simulation principles were
applied in both SMCS procedures.

253 B. Initialization Module

254 The initialization module is used to calculate several quan-
255 tities required by the main simulation loop. Following the
256 data input, network model with real-time thermal ratings and
257 load customer characteristics is built and fed into the first
258 SMCS procedure, as shown in Fig. 1. The outputs from this
259 stage are some pricing and reliability indicators.

1) *Input Data*: The input data include network, reliabil-
ity, customer, economic data, overhead line (OHL) data and
weather data. Beside the standard network data, forecast in-
service generation units with technical characteristics and
chronological hourly load point demands are input. Reliability
data are failure rates and repair times of all components, whilst
customer data encompass customer and DR types, contracted
voluntary load reductions, normalized load recovery profiles
and customer availability to respond to a DR call. Essential
economic data are generation costs, values of lost load (VOLL)
and marginal offer prices for voluntary load reduction. Average
VOLL data by customer types were obtained from the latest
U.K. national study [13].

Weather data include ambient temperatures, wind speeds
and directions required for the calculation of RTTRs of OHLs,
as well as either forecast hourly wind speeds or hourly wind
speed PDFs used to calculate wind generations. Several other

277 OHL construction and heat dissipation/gain data are further
278 required to calculate RTTRs.

279 The input data are fed into the thermal ratings and network
280 modelling modules, whose outputs are then used by the SMCS
281 procedures.

282 2) *Thermal Ratings of Overhead Lines*: Two different OHL
283 rating models are used in the developed simulation proce-
284 dures, the ‘seasonal’ thermal rating (STR) and the RTTR. The
285 STR is defined by seasons and for different design conductor
286 temperatures [14]. The lowest ratings are for summer con-
287 ditions and design temperature of 50°C [15]; they are of
288 conservative nature.

289 To get the RTTRs, it is possible to do a thermal analysis on
290 an hourly basis. Assuming a steady-state thermal equilibrium
291 is achieved in each hourly period, static thermal balance is
292 achieved by equating heat dissipated by convection and radi-
293 ation (or ‘cooling’) with solar and Joule heat generated. In
294 the applied IEEE model [15], the convection heat loss varies
295 with the change in wind speed (V_m), wind direction factor
296 (K_{angle}) and the difference between the conductor (T_c) and
297 ambient air temperature (T_a). The radiation heat loss is the
298 energy of the electromagnetic waves emitted to the ambient
299 space; it is a function of the temperature difference between
300 the conductor and air, and the emissivity of the conductor. The
301 solar radiation is a function of several parameters including
302 solar azimuth, total radiated heat flux rate, etc. Finally, Joule
303 (I^2R) losses are calculated in the standard way using AC resis-
304 tance dependent on conductor temperature, so that the RTTR
305 of OHLs is determined as:

$$306 \quad I = \sqrt{(P_c(T_c, T_a, K_{angle}, V_m) + P_r(T_a, T_c) - P_s) / R(T_c)} \quad (1)$$

307 where $P_c(\cdot)$ is the convection heat loss, $P_r(\cdot)$ is the radiated
308 heat loss, P_s is solar heat gain and $R(T_c)$ is the conductor
309 resistance at operating temperature T_c . The conductor temper-
310 ature needs to be set to one of the standard design values
311 (i.e., 50°C, or 65°C, or 75°C) to get the OHL ampacity; an
312 increased value can be used during system emergencies.

313 The average values of 5-year hourly weather data were
314 obtained from the BADC MIDAS meteorological stations for
315 Aonach, U.K. [16]. The rest of the required data were obtained
316 from the U.K. consultants.

317 3) *Analysis Within the SMCS Procedure*: The initialization
318 module is used for two purposes; the first is to determine
319 the base expected duration interruption (BEDI) index of loads
320 needed for ranking of loads within the demand reduction
321 scale module. The second is to compute the probabilistic
322 energy nodal prices used within the DRLR-control module
323 to find the optimal load recovery strategy. The probabilistic
324 nodal prices at different confidence intervals α are further
325 analysed to make decision about the most appropriate load
326 recovery times.

327 Each hour within the simulation period is characterized by
328 available generating units, transformers and circuits, as well
329 as nodal loads and operational constraints. An optimum power
330 flow (OPF) model is solved to find the levels of voluntary
331 and involuntary load reductions and revenues to generator
332 and demand customers. The formulation of the OPF model is
333 a modification of the market-clearing model proposed in [17];

the main difference is that there is no preventive control 334
and corrective scheduling is applied to the already sampled 335
contingent case. Mathematical formulation of the model is: 336

$$337 \quad \text{Min} \left\{ \sum_{j \in J} C_{gj} \cdot P_{gj} + \sum_{i \in I} \sum_{s \in S} VOLL_i^s \cdot IVL_i^s \right. \\ \left. + \sum_{i \in I} \sum_{s \in S} \sigma_i^s \cdot VL_i^s \right\} \quad (2) \quad 338$$

$$339 \quad \text{subject to: } P_g - P_d - B\theta = 0 \quad (\mu) \quad (3) \quad 339$$

$$340 \quad P_f = H\theta \quad (4) \quad 340$$

$$341 \quad -P_f^{\max} \leq P_f \leq P_f^{\max} \quad (5) \quad 341$$

$$342 \quad -P_g^{\min} \leq P_g \leq P_g^{\max} \quad (6) \quad 342$$

$$343 \quad 0 \leq VL_i^s \leq VL_i^{s, \max} \quad (7) \quad 343$$

$$344 \quad 0 \leq IVL_i^s \leq IVL_i^{s, \max} - VL_i^{s, \max} \quad (8) \quad 344$$

$$345 \quad P_d^{\max} - \sum_s IVL^s - \sum_s VL^s \leq P_d \leq P_d^{\max} \quad (9) \quad 345$$

346 The objective function to be minimized (2) is the sum of
347 the offered cost functions for generating power plus the sum
348 of the cost of involuntary load reduction for all load nodes
349 and types plus the sum of offered costs for voluntary load
350 reduction for all load nodes and types. The involuntary load
351 reduction is valued at $VOLL$ that is dependent on the general
352 load type; dependency on the connection node is taken into
353 account because there may exist special loads whose curtail-
354 ment must be avoided. Voluntary load reduction is priced at
355 the rates offered by consumers to provide this service. They
356 are closely linked to the offers made by generators for the ‘up-
357 spinning reserve’ in the joint energy and reserve market [17].
358 It is again envisaged that the rates can vary with customer
359 type and connection location. Finally, note that time index t
360 is avoided for simplicity.

361 Using a dc load flow model, constraints (3) represent the
362 nodal power balance equations for the considered state, which
363 includes potential contingencies within the system matrix B .
364 A Lagrange multiplier (or dual variable) μ_i is associated with
365 each of the equations. Constraints (4) express the branch flows
366 in terms of the nodal phase angles, while constraints (5)
367 enforce the corresponding branch flow capacity limits. Here,
368 modelling of OHL ratings can be done using the RTTR model,
369 in which case limit P_f^{\max} is a function of the time step t .

370 Constraints (6) set the generation limits for the consid-
371 ered state, while considering available units and requirements
372 for the down- and up-spinning reserve in the analysed time
373 step [17]. Reserve requirements depend on the system load and
374 contingency state [17]. For the non-controllable units, such as
375 wind turbines, upper and lower limits are the same.

376 Constraints (7), (8) and (9) set the limits of the demand; they
377 are expressed as inequality constraints on the voluntary and
378 involuntary load reductions and the total delivered load. The
379 upper limit of the voluntary load reduction $VL_i^{s, \max}$ can contain
380 a probabilistic component for some DR types and is dependent
381 on the considered time step. As a consequence, the upper limit
382 of the involuntary load reduction is the difference between of
383 the absolute limit $IVL_i^{s, \max}$ and the voluntary load reduction

384 limit $VL_i^{s,max}$. Finally, the delivered demand P_d is equal to
 385 the forecast load in the considered time interval P_d^{max} if there
 386 is no load reduction. The lower limit is specified in terms of
 387 the forecast load, voluntary and involuntary load reductions,
 388 which are a part of the optimal solution.

389 Solving the optimization model (2) to (9) gives the optimal
 390 values of the unknown variables, as well as dual variables
 391 associated with the constraints of this problem [18]. The
 392 significance of the dual variables is discussed below.

393 4) *Nodal Marginal Costs*: The optimal solution of the
 394 problem (2) to (9) is equal to the optimal solution of the cor-
 395 responding dual problem whose unknowns are dual variables
 396 associated with the constraints (3) to (9) [18]. The objective
 397 function of the dual problem is a sum of products of the dual
 398 variables and the right-hand sides of the constraints, showing
 399 that the total optimal cost can be recovered in another way
 400 using the dual variables as charging rates. The dual variables
 401 represent the additional cost of changing the right-hand side
 402 of the constraints by unity; they are therefore called marginal
 403 costs or prices [19].

404 Dual variables μ are the nodal marginal costs of meeting the
 405 power balance at each system node for the considered oper-
 406 ating regime. The nodal marginal costs have been extensively
 407 used for electricity energy and reserve pricing [6], [9], [20].
 408 The nodal marginal prices vary over the system nodes and
 409 during the day due to load variation and congestion in the
 410 system [21]. The greatest variation of marginal prices is
 411 experienced due to unexpected failures of lines and/or gener-
 412 ator units [6]. Consequently, these prices should be carefully
 413 considered for the load recovery scheduling.

414 In our approach, we have applied a concept similar to
 415 the real time pricing scheme proposed in [22]. The following
 416 quantities are calculated in each time step t :

- 417 • The revenue of generator j :

$$418 \quad GR_j(t) = Pg_j(t) \cdot \mu_j(t) \quad (10)$$

- 419 • The cost of demand i delivery:

$$420 \quad LC_i(t) = P_{di}(t) \cdot \mu_i(t) \quad (11)$$

- 421 • Revenue for voluntary load i reduction:

$$422 \quad VLR_i(t) = \sum_{s=1}^{s4} (\sigma_i^s(t) \cdot VL_i^s(t)) \quad (12)$$

- 423 • Revenue for involuntary load i reduction:

$$424 \quad IVLR_i(t) = \sum_{s=1}^{s4} (VOLL_i^s \cdot IVL_i^s(t)) \quad (13)$$

425 We have defined $VOLL$ by load types in the initialization mod-
 426 ule, as presented in equation (13). However, in the second
 427 SMCS there is an option to use a look-up table where $VOLLs$
 428 are functions of interruption duration [23]. The interruption
 429 duration is estimated as:

$$430 \quad D_i^s = \begin{cases} \text{mean}(D_i^s \text{ BASE}), & \text{if } D_i^s \leq \text{mean}(D_i^s \text{ BASE}) \\ D_i^s, & \text{if } D_i^s > \text{mean}(D_i^s \text{ BASE}) \end{cases} \quad (14)$$

431 where $D_i^s \text{ BASE}$ denotes the interruption duration calculated
 432 in the initialization module. The estimated duration of

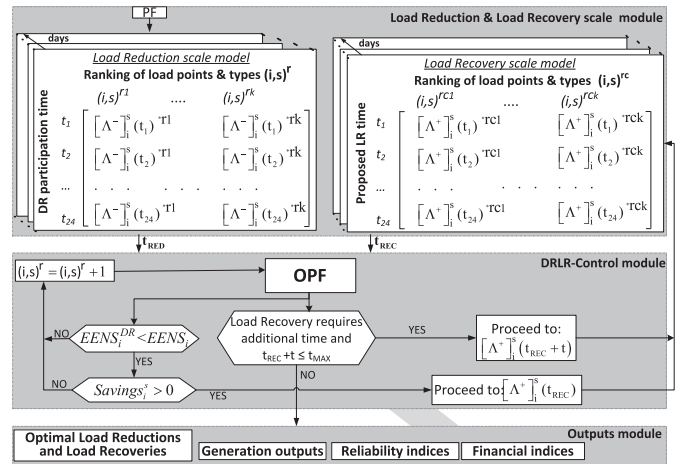


Fig. 2. Optimal demand response computational framework.

433 interruption is equal to the mean base value unless the inter-
 434 ruption already lasts for more than the base value; it then takes
 435 the actual duration value.

436 C. Optimal Demand Response Scheduling

437 The computational framework for optimal demand response
 438 scheduling is illustrated in Fig. 2. The load reduction and
 439 recovery scale modules feed into the DRLR control module.
 440 Ranking of different load types and calculation of *available*
 441 sizes for voluntary load reduction is performed within the load
 442 reduction scale module. The order of ranking the load points
 443 and types is represented by $(i, s)^r$ in Fig. 2. Hence, in the load
 444 reduction matrix, if load reduction takes places at hour t_j the
 445 load reduction of $(i, s)^r$ customer will be evaluated first, while
 446 the $(i, s)^{rk}$ customer will be evaluated at the end.

447 The load recovery scale module computes the most appro-
 448 priate schedule hours for load recovery, as well as the potential
 449 recovery sizes and profiles. The order of ranking the load
 450 points and types is represented by $(i, s)^c$ in Fig. 2. Hence, in
 451 the load recovery matrix, if load recovery takes places at hour
 452 t_j the load reduction of $(i, s)^{rc1}$ customer will be evaluated
 453 first, while the $(i, s)^{rc2}$ customer will be evaluated at the end.
 454 Both load reduction and recovery are managed by the DRLR
 455 control module in which the OPF is used to determine optimal
 456 voluntary and involuntary load reductions, and the developed
 457 control scheme gives the optimal load recovery profiles. The
 458 outputs module finally gives optimal DR and LR schedules,
 459 as well as financial and reliability indicators.

460 D. Load Reduction Scale Module

461 Load reduction scale module is required for each load point
 462 and load type when load shedding takes place at the considered
 463 hour t_{RED} . The physics of demand response are presented first,
 464 which is followed by the ranking and sizing.

465 Four load types, industrial, commercial, large user and
 466 residential, have been defined in our approach. Different
 467 characteristics have been associated with these four types,
 468 such as temporal load variations, total amounts available for

voluntary and involuntary load reductions, relative load recovery profiles and economic data. Two categories of demand response have been recognised, namely direct and indirect load control [24]. In direct load control, the contracted customers (usually large and industrial) are directly disconnected during emergency conditions and they receive revenue for participating in the ‘reserve market’ [25]. The contracted amounts are certain and they are of deterministic nature. In indirect load control, incentive- and price-based demand responses can be distinguished. The former group refers to the customers contractually incentivised to curtail load during system emergencies [26], [27]. This category can be considered semi-probabilistic; we have used sampling within a window around the contracted value. Finally, in price based demand response customers move their consumption from periods of higher to periods of lower prices. This demand response is a probabilistic quantity which can vary from zero up to the estimated maximum amount.

Load ranking at each node i and for each load type s at the considered hour t_{RED} is based on the financial implications of reducing the load. The ranking order is a product of the normalized value of the base expected duration interruption index ($BEDI_i$) calculated in the initialization module, the normalized marginal offer price $\hat{\sigma}_i^s$ for voluntary load reduction or customer interruption cost $VOLL_i^s$ for involuntary load reduction, and the required load shedding Pc_i^s . This is shown in relations below:

$$\hat{R}_i^s(t_{RED}) = \begin{cases} \hat{B}EDI_i \cdot Pc_i^s \cdot \hat{\sigma}_i^s, & \text{voluntary load} \\ \hat{B}EDI_i \cdot Pc_i^s \cdot VOLL_i^s, & \text{involuntary load} \end{cases} \quad (15)$$

$$BEDI_i = \sum_{y=1}^Y \sum_{t=1}^T \sum_{s=1}^{s_4} \zeta_i^s \cdot D_i^{BASE} / Y \quad (16)$$

Relation (15) shows that independent ranking lists for voluntary and involuntary load reductions can be built. Ranking of all ‘voluntary customers’ is based on submitted marginal offer prices, which can be normalised with the average price of up-spinning reserve in the energy-reserve markets [17]. On the other hand, involuntary load reductions are ranked using $VOLL$. The $VOLL$ is defined either by load types, or customer damage functions are used; it is normalised using the average $VOLL$ in the entire GB [13]. The base expected interruption index $BEDI_i$ is found from the number of interruptions ζ_i^s having duration D_i^{BASE} across the entire simulation period.

The total required amount of load reduction Pc_i^s is determined from the OPF model and it consists of voluntary and involuntary components. When considering industrial and large customers under the direct load control, it was assumed that available voluntary load reduction is equal to the contracted voluntary reduction (CVL_i^s). Then the (part of) voluntary load reduction is:

$$[\Lambda^-]_i^s(t_{RED}) = \begin{cases} Pc_i^s(t), & \text{if } Pc_i^s(t) < CVL_i^s(t) \\ CVL_i^s(t), & \text{if } Pc_i^s(t) > CVL_i^s(t) \end{cases} \quad (17)$$

Available voluntary load reductions from industrial and commercial incentivised customers and residential customers contain a probabilistic component that can be determined using random sampling. It is calculated using the availability

factor f_{RED}^s :

$$f_{RED}^s = \begin{cases} 1 + (rs - 1)win, & \text{industrial \& commercial} \\ rs, & \text{domestic customers} \end{cases} \quad (18)$$

where rs is a random number generated from the uniform distribution between $\{0,1\}$ and win is the per unit window. In case of incentivised (industrial and commercial) customers, the available amount is based on average probability that the contracted amount is available; for example, if the probability is 0.9 then $win=0.2$. Residential customers respond to price signals and the uncertainty window is the entire available range. The available voluntary load reduction is then calculated by multiplying the availability factor (18) and the contracted value (CVL_i^s) in case of incentivised industrial and commercial customers, or estimated maximum load reduction of residential customers.

After having obtained *available* voluntary load reductions for all types of customers s at node i , the total voluntary and involuntary load reductions are calculated using the ranking order and a relation similar to expression (17). The minimum amount of involuntary load reduction is always used to meet the network security constraints.

E. Load Recovery Scale Module

This module determines the amounts of *potential* load recoveries in the period following load reduction in time slot t_{RED} . The actual load recovery is determined in the DRLR control module using the hourly nodal marginal prices.

Load recovery profiles can be very different for the considered customer types, and moreover, for different customers within a single group; a good example is industry [28]. We applied a general normalized load recovery profile of triangular shape, which is modelled by two straight lines in discrete form. The upward line models load pick-up after the customer reconnection, whilst the downward line brings it back from the ‘overshot point’ to the pre-disconnection value. The discrete modelling is done using the upward/downward slope coefficients in consecutive time intervals.

The amount of load recovery at time period $t_{REC} + t$, $[\Lambda^+]_i^s(t_{REC} + t)$, is computed by using the following expression:

$$[\Lambda^+]_i^s(t_{REC} + t) = [\Lambda^-]_i^s(t_{RED}) \cdot \gamma_i^s(t_{REC} + t) \cdot f_{REC}^s \quad (19)$$

where $[\Lambda^-]_i^s(t_{RED})$ is amount of load reduction of load type s at node i , $\gamma_i^s(t_{REC} + t)$ is upward or downward slope coefficient and f_{REC}^s is the availability factor of type s load recovery. This factor was introduced because not all customers may come back when supplies are restored or signalled [29]. In the current approach, availability factors f_{REC} are deterministic quantities defined by customer types and network nodes. It is also worth noting that the load recovery can be higher than the amount of the initial load reduction [28]; the slope factors can take values greater than unity.

Modelling of load recovery profiles over a specified time period introduces additional complexities in the developed SMCS methodology. Each time a load recovery is initiated, the corresponding nodal load needs to be modified over a specified

574 period in line with the load recovery profile. Besides, a record
575 must be kept of all load recoveries at different time steps,
576 because they cannot be considered for further load reduction.
577 This is reflected in the next DRLR module.

578 F. Demand Reduction Load Recovery Control Module

579 The DRLR control module is used to control the initiation
580 of load reductions and recoveries and to produce their optimal
581 schedules within the forecast 24 hourly period. Some of the
582 control principles are listed below:

- 583 • Loads whose recovery process is underway cannot be
584 considered for load reduction.
- 585 • Loads eligible for load reduction will not be disconnected
586 if there is no improvement in the energy-not-served
587 following the load reduction.
- 588 • Only those loads, whose reduction including recovery
589 generates revenue to the customers, will be actually
590 disconnected and reconnected.
- 591 • The best timing of load recovery is determined using
592 the (forecast) nodal marginal prices over the recovery
593 period.

594 Assume the OPF analysis has generated non-zero load cur-
595 tailments. Those loads which are not a part of previous load
596 recoveries are ranked and sizes of voluntary and involuntary
597 reductions are determined. The first load reduction from the
598 ranking list is applied and it is checked with the aid of the
599 OPF whether the total energy-not-served has reduced. If this
600 is the case, the nodal customer *profits* are computed based on
601 the *savings* acquired due to the load reduction and the pro-
602 jected *payback cost* due to the load recovery. The optimum
603 load recovery always takes place when the nodal marginal
604 prices are ‘low’ over the recovery window. If the load cus-
605 tomer projected profit is negative, the load reduction is not
606 activated even if the reliability of the network might improve.

607 Calculation of customer savings, costs and profits is briefly
608 presented below.

609 1) *Customer Savings*: The customer savings incurred dur-
610 ing load reduction are the consequence of reduced load
611 payments to the generators. These payments are valued at
612 nodal marginal prices $\mu_i(t)$, as shown in equation (11), which
613 are in turn dependent on the considered regime. The customer
614 savings are therefore calculated from two OPF runs: the first
615 without load reduction and the second with load reduction.
616 The change in load payments, ΔLC , represents the customer
617 savings at t_{RED} :

$$618 \quad \Delta LC_i^s(t_{RED}) = LC_i^{s\ NO-DR}(t_{RED}) - LC_i^{s\ DR}(t_{RED}) \quad (20)$$

619 The total savings are then found for the entire interval when
620 the load reduction is in place:

$$621 \quad Savings_i^s(t_{RED}) = \sum_{t=t_{RED}}^{t_{REC}} \Delta LC_i^s(t) \quad (21)$$

622 2) *Payback Costs*: If customer *savings* are positive then the
623 algorithm proceeds to the load recovery stage to project the
624 optimal load recovery schedule. The optimization is based on
625 the following principles:

- Load recovery is always scheduled after the correspond- 626
ing load reduction and it can continue into the ‘following’ 627
simulated day. There are periods within a day when the 628
load recovery does not take place; for example between 629
12am and 5pm on weekdays for residential customers. 630
- Load recovery blocks due to involuntary load reduction 631
are always committed before voluntary load recovery 632
blocks. They are prioritized based on their VOLL; where 633
the VOLL is the same, ranking is based on the size of 634
load reduction, the largest loads being reconnected first. 635
Similar criteria are applied to voluntary load reductions, 636
where marginal offer prices are used instead of VOLL. 637
- Optimal timing of load recovery is determined by find- 638
ing the weighted average of (base) nodal marginal prices 639
over the recovery window. The weights are equal to the 640
slope coefficients $\gamma_i^s(t_{REC} + t)$ of the normalized recov- 641
ery profile. The window with the smallest average nodal 642
marginal price is selected for the load recovery. This 643
approach is the best for load customers, because they 644
will be exposed to the least additional payback cost. 645
- After having determined the optimal starting hour of load 646
recovery, it will only be materialized if there will be no 647
new load curtailments within the recovery window. This 648
is checked by running OPF over consecutive time periods 649
within the recovery window; where curtailments occur, 650
the next best recovery window is examined and so on. 651

The payback costs due to the selected optimal load recovery 652
schedule are again computed from two OPF runs in each time 653
step within the recovery window. Since load recovery increases 654
the amount of load, additional cost ΔLC is calculated as the 655
difference between costs with and without load recovery over 656
the load recovery period t_{REC} to t_{MAX} : 657

$$\Delta LC_i^s(t_{REC}) = LC_i^{s\ DR}(t_{REC}) - LC_i^{s\ NO-DR}(t_{REC}) \quad (22) \quad 658$$

$$C_{payback\ i}^s = \sum_{t=t_{REC}}^{t_{MAX}} \Delta LC_i^s(t) \quad (23) \quad 659$$

3) *Customer Profits*: The total customer profit $\pi_i^s(t_{RED})$ 660
needs to account for savings due to reduced load, costs due to 661
load recovery, as well as rewards for voluntary and involuntary 662
load shedding. This is summarised in the equation below: 663

$$664 \quad \pi_i^s(t_{RED}) = Savings_i^s - C_{payback\ i}^s + \sum_{t=t_{RED}}^{t_{REC}} IVLR_i^s(t) \quad 664$$

$$+ \sum_{t=t_{RED}}^{t_{REC}} VLR_i^s(t) \quad (24) \quad 665$$

Only load customer with a positive profit $\pi_i^s(t_{RED})$ evaluated 666
at time t_{REC} proceeds into the DR strategy. The analysis con- 667
tinues until the convergence criterion on expected energy not 668
served is met. After having completed the SMCS procedure, 669
the algorithm goes straight to the outputs module. 670

671 G. Outputs Module

The outputs module generates several results related to the 672
load reductions, nodal prices, generation outputs, reliability 673
and financial indicators. They are briefly discussed below. 674

675 1) *Optimal Load Reductions and Recoveries*: PDFs of vol-
 676 untary and involuntary load reductions by load types and/or
 677 nodes are calculated for each hour in the 24-hourly period.
 678 These can be directly converted into energy not served PDFs.
 679 The corresponding mean and percentile values show the
 680 ‘likely’ distributions in the next 24-hourly period. PDFs of
 681 daily totals are also computed. Besides, conditional PDFs of
 682 the load recovery initiation times given the load reduction at
 683 certain hour are also produced.

684 2) *Generation Outputs*: PDFs of generator hourly produc-
 685 tions and costs, as well as total daily costs are computed.

686 3) *Nodal Marginal Prices*: PDFs of nodal marginal prices
 687 are produced for each hour in the considered 24-hourly period.
 688 Their expectations can be used as an indicator what the prices
 689 for rewarding generation and charging load customers will be
 690 next day.

691 4) *Reliability Indices*: Reliability indices relating to energy
 692 not served as well as frequency of customer interruptions and
 693 duration of interruptions are computed. For example, expected
 694 energy not supplied (*EENS*), expected frequency of interrup-
 695 tions (*EFI*) and expected duration of interruptions (*EDI*) are
 696 calculated as:

$$\begin{aligned}
 697 \quad EENS &= \sum_{y=1}^Y \sum_{t=1}^T \sum_{i=1}^N \sum_{s=1}^{s_4} P c_i^s / Y, \\
 698 \quad EFI &= \sum_{y=1}^Y \sum_{t=1}^T \sum_{i=1}^N \sum_{s=1}^{s_4} \xi_i^s / Y \\
 699 \quad EDI &= \sum_{y=1}^Y \sum_{t=1}^T \sum_{i=1}^N \sum_{s=1}^{s_4} \xi_i^s \cdot D_i^s / Y. \quad (25)
 \end{aligned}$$

700 5) *Financial Indicators*: PDFs of load customer pay-
 701 ments (*LC*), voluntary (*VLR*) and involuntary load reduction
 702 rewards (*IVLR*) are computed by hours and for the considered
 703 day. The latter curves are then used to quantify the financial
 704 risk of implementing the proposed demand response schedul-
 705 ing. The concept of value-at-risk (*VaR*) [30] was applied
 706 to measure the potentially ‘low’ revenues or ‘excessive’
 707 payments.

708 Assuming network reward (*NR*) denotes any category of
 709 revenues, the corresponding cumulative distribution func-
 710 tion (CDF_{NR}) is used to calculate the network reward NR_X
 711 that exceeds the network reward at the confidence level α ,
 712 NR_α , with probability $1 - \alpha$. The value at risk is [31]:

$$713 \quad VaR_\alpha^{NR}(NR_X) = \inf\{NR_\alpha \in \mathbb{R} : CDF_{NR_X}(NR_\alpha) \geq \alpha\} \quad (26)$$

714 Similarly, the *CDF* of any network cost (*NC*) can be used
 715 to determine value-at-risk at confidence level α . In this case,
 716 network cost NC_X that does not exceed the network cost at
 717 probability $1 - \alpha$, $NC_{1-\alpha}$, is calculated as:

$$718 \quad VaR_{1-\alpha}^{NC}(NC_X) \\
 719 \quad = \sup\{NC_{1-\alpha} \in \mathbb{R} : CDF_{NC_X}(NC_{1-\alpha}) \leq 1 - \alpha\}. \quad (27)$$

720 IV. BULK ELECTRIC POWER SYSTEM

721 This section describes some practical aspects of the ampac-
 722 ity calculation of OHLs, modelling of wind farms, as well as
 723 the designed case studies.

TABLE I
 CONDUCTOR PROPERTIES MODELED IN IEEE-RTS NETWORK

NAME	<i>Rac</i> (Ω/Km)	<i>Configuration</i>	<i>S_{NORM}</i> (<i>MVA</i>)	<i>S_{EM-LONG}</i> (<i>MVA</i>)
Dove (138kV)	0.1003 @ 25°C 0.1270 @ 75°C	Single bundle	95 [60°C]	138 [75°C]
Hawk (230kV)	0.1154 @ 25°C 0.1225 @ 75°C	Twin bundle	308 [60°C]	365 [75°C]

724 A. Thermal Ratings of Overhead Lines

725 The IEEE-RTS 96 test system does not provide any OHL
 726 data required for the RTTR calculations. A simple ACSR tech-
 727 nology was assumed with conductor sizes that provide similar
 728 ratings to those in the IEEE-RTS 96 system with AAAC and
 729 ACSR conductors. Table I provides the information on the con-
 730 ductors used in the analysis. Under normal operation conductor
 731 temperature, T_c , is set to 60°C. A line is considered in emer-
 732 gency state when another transmission line connected at the
 733 same bus fails. The maximum conductor temperature in emer-
 734 gencies is set to 75°C based on avoidance of the conductor
 735 annealing [32].

736 B. Integration of Wind Farms

737 The power output of a wind turbine generator (WTG) is
 738 driven by the wind speed and the corresponding relationship is
 739 nonlinear. It can be described using the operational parameters
 740 of the WTG, such as cut-in, rated and cut out wind speeds.
 741 The hourly power output is obtained from the simulated hourly
 742 wind speed using the relations [33]:

$$\begin{aligned}
 743 \quad P(V_m) \\
 744 \quad = \begin{cases} 0, & 0 \leq V_m < V_{ci} \\ (A + B \times V_m + C \times V_m^2) \times P_r, & V_{ci} \leq V_m < V_r \\ P_r, & V_r \leq V_m < V_{co} \\ 0, & V_m \geq V_{co} \end{cases} \quad (28) \\
 745
 \end{aligned}$$

746 where P_r , V_{ci} , V_r , and V_{co} are, respectively, rated power out-
 747 put, cut-in wind speed, rated wind speed and cut-out wind
 748 speed of the WTG, whilst V_m is simulated wind speed at
 749 hour t . The power output constants A , B and C are determined
 750 by V_{ci} , V_r , and V_{co} , as shown in [33]. All WTG units used
 751 in this study are assumed to have cut-in, rated, and cut-out
 752 speeds of 14.4, 36, and 80km/h, respectively. The failure rates
 753 and average repair times are assumed to be two failures/year
 754 and 44 hours.

755 C. Case Study Description

756 OHL thermal ratings are modelled as STR or RTTR, as
 757 shown in Table II below. Three seasons (winter, summer and
 758 fall), denoted as $\lambda_s = 1, 2, 3$, are studied. The first day of
 759 the 50th peak week of the year is used for winter (hours:
 760 8425-8449); the 2nd day of the 22nd week of the year is
 761 used for summer (hours: 3721-3744) and the 2nd day of the
 762 32nd week is used for fall (hours: 5401-5424). Availability
 763 factor f_{RED}^s is a random number, whilst availability factor
 764 for load recovery f_{REC}^s varies in the specified range. Load

TABLE II
MODELING SCENARIOS OF DR METHODOLOGY

	S1	S2	S3	S4	S5	S6	S7	S8
p	STR	STR	STR	STR	RTTR	RTTR	STR	STR
λ_s	1,2,3	1	1,2,3	1	1	1	1	1
f_{RED}^s	0	1	1	1	0	1	0	1
f_{REC}^s	0	1	1	0-1.2	0	1	0	1
ϑ_{REC}	-	0	1	1	-	1	-	1
wg	0	0	0	0	0	0	1	1

recovery is based on either hourly emergency energy prices (i.e., $\vartheta_{REC} = 1$) or load profiles (i.e., $\vartheta_{REC} = 0$). The presence of wind generators is denoted by $wg=1$.

Eight scenarios are described in Table II. Scenario S1 is the base case, where the system is evaluated without DR scheduling and with standard thermal ratings for OHLs. Scenario S2 models load recovery by using the hourly load curve at each load point ($\vartheta_{REC} = 0$). Scenario S3 models all seasons and load recovery on the basis of expected marginal prices at each load point ($\vartheta_{REC} = 1$). Scenario S4 models time-varying load recovery profiles. Sensitivity studies are done here in order to assess the impact of different recovery sizes and profiles on DR performance. Factor f_{REC}^s is set from 0 to 1.2pu increasing in 0.2pu increments; the 1.2pu is taken as a high-risk scenario. Scenario S5 incorporates the RTTR of OHLs without DR operation, while Scenario S6 includes the DR scheduling. Finally, Scenario S7 incorporates wind farms without DR, while in Scenario S8 the benefits of demand response are evaluated incorporating wind generation ($wg=1$).

The original IEEE-RTS 96 was modified: all scenarios assume an increase in load by 1.2pu compared to the original load, as well as increase of 0.55pu and 0.6pu transmission capacity for the 138kV and 230kV levels, respectively, and 1.2pu in generation capacity. Next, the WTGs are connected at seven sites and it was assumed that they operate at power factor mode with power factor equal 35% [34]. Wind farms are designed to deliver 20% of the peak load [35], equivalent to 684MW on the studied power network. Geographically, 70% of the wind farms' maximum capacity is installed in the northern part of the network at buses 15, 17, 19, 20, 22, while in the southern part of the network, the remaining 30% of the wind capacity is installed to at buses 1, 2, 7, 8. The total wind farm capacity is 2394 MW obtained from a total number of 240 WTG, each representing a nominal capacity of 10MW. There is significant transmission utilization in this modified system as the bulk of the generating capacity is located mainly in the northern areas and considerable power is transferred from the north to the south aiming to represent the existing topology of the U.K. network. The analysis will study potential low wind output conditions in combination with unexpected network components failures.

V. CASE STUDY ANALYSIS

The IEEE-RTS 96 is composed of 38 lines circuits, 32 generating units and 17 load delivery points [36].

It is studied by using the algorithms developed in Matlab that make use of a modified version of Matpower and MIPS

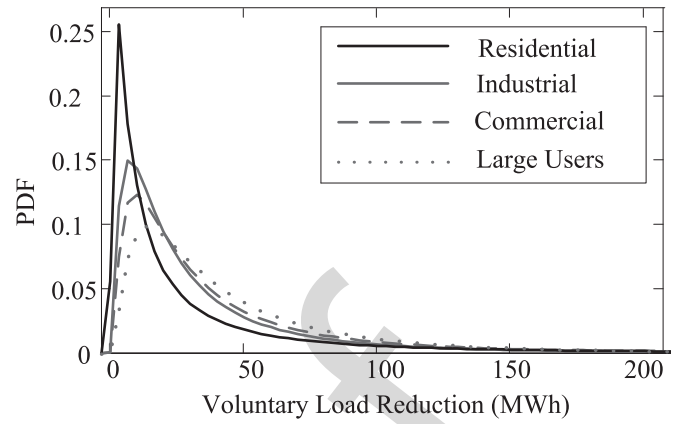


Fig. 3. Probability to respond to a DR signal for different customer types based on the voluntary load reduction amount at 17h00.

solver for the power flow calculations [37]. Essential study results on the eight scenarios related to the availability for load reduction, impact of nodal marginal prices, load recovery profile – availability, and impact of RTTR, DR and wind generation, are presented below.

A. Customer Availability for Load Reductions

In this section, the impact of the availability of customers responding to a DR call is examined. Uncertainty in load availability for each customer type is given by equation (18). In particular, domestic customers' load reduction takes values from the entire possible range, while for industrial and commercial loads it is within the assumed window, $win=0.8-1pu$. Scenario 3 (S3) is used to evaluate the impact of customers responding to a DR on the *EENS*, mean and *Var* values of voluntary (VLR) and involuntary load reductions (IVLR) – eqs. (12) and (13). For VLRs, Fig. 3 (generated over the entire MCS period) shows that the probability for residential loads to give 'small' response (up to 25 MWh) is much higher than to produce 'large' response (up to 50MWh).

However, industrial, commercial and large users are more likely to give 'larger' responses as they have bigger contracted amounts compared to residential users, and the uncertainty in response (if any) is much lower. For low load reductions, industrial loads have higher probability to respond than commercial and large users, while large users have the highest probability for larger amounts of load reductions; they are followed by commercial and industrial users.

The PDFs for voluntary (VL) and involuntary (IVL) load reductions for different hours in a day are illustrated in Fig. 4 and compared with the PDF of IVL without DR ($IVL^{NO\ DR}$). The results show that the probability of having IVL is reduced when doing DR (IVL^{DR}) with higher amounts (right side of x-axis), while the probability is much higher for low amounts of IVL. This clearly shows the effectiveness of voluntary DR on the *EENS*. In particular, the mean value of IVL^{DR} at 17h00 is around 60% less than the mean value of $IVL^{NO\ DR}$. A similar conclusion applies to all hours; for example, the mean of IVL^{DR} at 21h00 and 22h00 is, respectively, 61% and 60% lower when applying the voluntary DR. Applying

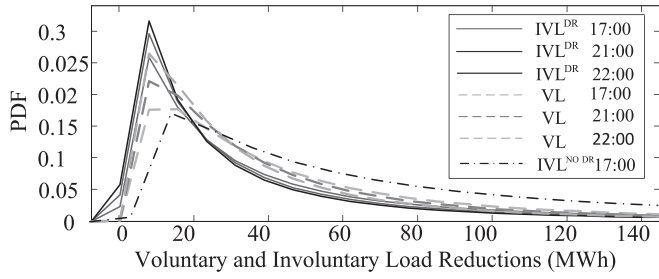


Fig. 4. Probability of voluntary and involuntary load reductions under DR for different hours in a day.

TABLE III
VAR VALUES OF CUSTOMERS COSTS AND REWARDS (k£)

Critical buses	B6		B8		B14	
	S1	S3	S1	S3	S1	S3
VaR _{50%} ^{LC}	31.43	19.59	55.13	22.91	57.55	41.72
VaR _{90%} ^{LC}	55.64	52.81	75.11	61.24	95.39	89.08
VaR _{50%} ^{VLR}	-	1.3	-	1.8	-	1.5
VaR _{90%} ^{VLR}	-	5.6	-	2.5	-	2.8
VaR _{50%} ^{IVLR}	600	240	578	320	480	252
VaR _{90%} ^{IVLR}	1344	420	1260	604	1284	546

voluntary load reduction (VL) helps eliminate the need for involuntary one (IVL^{NO DR}), particularly when larger VL amounts are used. This is further highlighted when converting VL and IVL into the EENS index (see Table IV in Section V-B).

Table III shows the mean (VaR_{50%}) and the 90% confidence VaR (VaR_{90%}) for the costs for demand (LC), for VLR and IVLR revenues for the most critical load points (B6, B8 and B14) under scenarios S1 and S3. Both the VaR_{50%}^{LC} and VaR_{90%}^{LC} are much lower under S3 for all load points, since under DR, demand is recovered under cheaper nodal marginal prices.

In addition, VaR_{90%}^{VLR} is much larger than VaR_{50%}^{VLR} since marginal nodal prices are significantly higher under emergency conditions. Furthermore, the VaR_{50%}^{IVLR} is much lower under S3 than under S1, where it decreases by 60% for B6, 44% for B8 and 47% for B14. This also shows that voluntary DR significantly decreases the need for IVL (an average VOLL value was assumed for all customer types).

B. Impact of Nodal Prices on Reliability Analysis

Most DR studies would recover reduced load during load troughs and/or system normal if only network adequacy were looked at.

However, we have used the approach to investigate impact of hourly nodal prices on load recovery and customers' well-being. Fig. 5 shows an example of the nodal marginal price and the demand variation in time for the most frequently interrupted bus in the network (B6) under both intact and emergency conditions.

When no failures occur, load can be recovered almost at any time since intact prices do not change significantly with

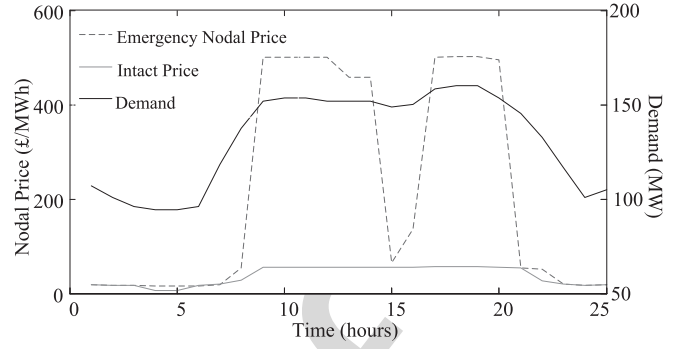


Fig. 5. Hourly marginal prices and demand curve under emergency for Bus 6.

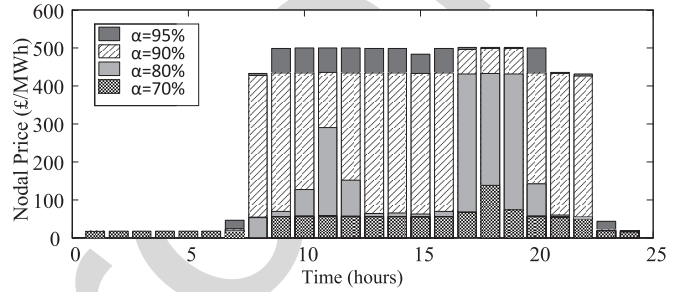


Fig. 6. Emergency marginal price for different confidence levels.

respect to load. However, nodal prices under emergency conditions may vary considerably. For instance, a significant shape difference between intact and emergency nodal prices is shown at 15h00. Our analysis has proven that the magnitude of the emergency nodal price can be almost 5 times higher than the intact one. Thus, scheduling of 'optimal' load recoveries based on marginal nodal prices has proven effective in providing system security and customer benefits. Furthermore, comparative studies were conducted to quantify the improvements from implementing load recovery under nodal marginal prices rather than under load profile only.

The hourly nodal price at bus B6 for different confidence levels is given in Fig. 6. In the event of an emergency at B6, TSOs may be provided with the illustrated confidence level dependent prices to decide which load recovery hour would be the most appropriate to restore load. For example, the TSO can know that if a violation occurs at 11h00, the load can be recovered between 13h00 and 16h00, since there is an 80% probability that the price will be between zero and 90£/MWh and a 90% probability that the price will be between zero and 420£/MWh. In this paper, a conservative confidence level of $\alpha = 95%$ was selected. This gives flexibility to TSOs to apply operational decisions so they can guarantee making a profit for the demand customers for almost all nodal prices in the feasible range, since the load recovery will be at either the emergency nodal prices or (lower) intact prices.

The results presented in Table IV show that DR strategy under scenario S3 improves the reliability of the network in terms of EENS by 66% in winter ($\lambda_s = 1$) compared with S1, allowing for almost a 5% decrease in EENS compared to S2. The S3 strategy also substantially improves reliability indices

TABLE IV
RELIABILITY INDICES FOR SCENARIOS 1, 2 AND 3

S	EENS(MWh/day)			EDI(*10 ⁻² h/day)			EFI(int/day)		
	1	2	3	1	2	3	1	2	3
λ_s	1	2	3	1	2	3	1	2	3
S1	577	160.5	36.4	23.9	9.7	0.99	0.039	0.0156	0.00234
S2	206	59.2	12.9	23.2	9.2	0.57	0.0385	0.0154	0.00231
S3	196	42.8	4.8	23.3	8.5	0.35	0.0383	0.01532	0.00229

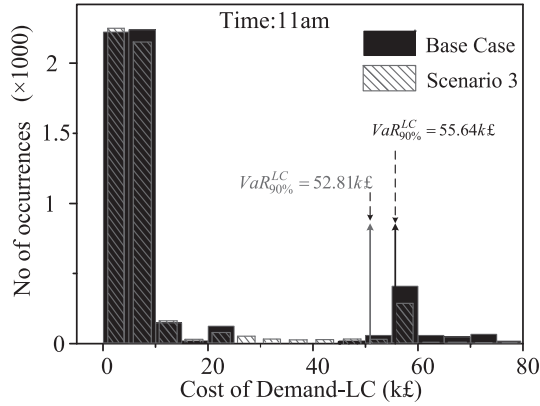


Fig. 7. Distribution of demand costs for load at Bus 6.

TABLE V
RELIABILITY INDICES FOR SCENARIO 4

f_{REC}^s (pu)	1.2	1	0.8	0.6	0.4	0.2
EENS(MWh/day)	205.8	196	192.34	191.13	191.08	188.12
EDI(h/day)	0.2334	0.2331	0.2330	0.229	0.227	0.227
EFI(int/day)	0.0386	0.0383	0.0383	0.038	0.038	0.0378

for summer ($\lambda_s = 2$) and fall ($\lambda_s = 3$), which demonstrates the effectiveness of the algorithm throughout the year.

In order to show the necessity to quantify the economic risk of DR operation, results for the base case S1 are compared to scenario S3 to investigate the VaR of the load cost (LC). Fig. 7 illustrates frequency of occurrence of various load costs seen at the most critical bus, B6, with and without DR. In particular, it is shown that there is a high variation in nodal costs at 11h00, resulting from outages of lines 12 and 13 that connect B6 with cheaper generators. Consequently, $VaR_{90\%}^{LC}$ is 55.64k£ under the base case, whereas it is only 52.81k£ under S3, which shows that DR can help reduce nodal costs by 5% (2.83k£). Clearly, both reliability and financial indices can be improved using nodal energy prices (S3) rather than the load profile only (S2).

C. Impact of Customer Availability to Recover the Load

The load recovery of a DR customer can be of different size compared to the corresponding load reduction. As a result, this can affect both the network performance and customer profits, as exemplified by scenario S4.

Assuming load recovery size is specified by availability factor f_{REC}^s , Table V shows an increase of around 5% in EENS for $f_{REC}^s = 1.2pu$ compared to $f_{REC}^s = 1pu$. When load recovery sizes are lower than 100%, network reliability is improved compared to $f_{REC}^s = 1pu$. This is due to the higher probability of implementing voluntary DR since less load recoveries

TABLE VI
DIFFERENCE IN MEAN AND VAR FOR LC (£) AND PROFITS (£/KWh) S4 VS. S3

S5	S4-S3 Values			
	$VaR_{50\%}^{LC}$	$VaR_{90\%}^{LC}$	$VaR_{50\%}^{\pi}$	$VaR_{90\%}^{\pi}$
$f_{REC}^s = 1.2$	+912	+1932	+0.05	+0.2
$f_{REC}^s = 0.8$	-89	+775	+5.3	+8.1
$f_{REC}^s = 0.6$	-101	-198	+6.3	+9.5
$f_{REC}^s = 0.4$	-257	-2102	+8.8	+9.5
$f_{REC}^s = 0.2$	-463	-2124	+10.2	+12.8

TABLE VII
IEEE RTS NETWORK EVALUATION WITH RTTR & DR

Reliability indices	Scenarios	S3	S5	S6
	EENS(MWh/day)		196	475
EFI (int/day)		0.0383	0.0381	0.0379
EDI*10 ⁻² (h/day)		23.31	23.34	23.18
Financial indices (k£)	$VaR_{50\%}^{LC}$	135.9	134.9	131.3
	$VaR_{90\%}^{LC}$	142.7	136.1	134.8
	$VaR_{50\%}^{VLR}$	1.6	-	1.2
	$VaR_{50\%}^{IVLR}$	2352	-	2196

are required. There is also a substantial decrease in reliability indices EDI and EFI.

Differences in the mean ($VaR_{50\%}$) and $VaR_{90\%}$ values for demand costs (LC) and customer profits (π) between scenarios S4 and S3 are shown in Table VI for different load recovery sizes f_{REC}^s . This table gives the cost and revenue differences following various load payback sizes compared to applying DR with a load payback of 100% for a winter day-ahead operation. For instance, when S4 is modeled with $f_{REC}^s = 1.2pu$, the $VaR_{50\%}^{LC}$ is 912£ higher than under scenario S3. This is because as load recovery gets larger, the operating conditions become more difficult and the marginal prices increase, implying higher costs for demand. For low load recovery sizes, however, very high profits can be incurred (over 2,100£) as the demand cost VaR shows the largest decrease, thus suggesting a much lower probability of high LC.

D. Impact of RTTR and DR on Network Reliability and Customer Costs & Revenues

In scenario S5 only RTTR is used, whilst scenario S6 makes use of DR in conjunction with RTTR. Table VII shows that the more reliable and cheapest scenario is S6.

The use of RTTR and DR under S6 results in, respectively, 61% and 6.6% reduction in EENS compared with DR alone (S3) and with S5. Indices EFI and EDI are also improved. When RTTR is considered alone (S5), the greater utilization of the three most critical lines improves network performance by 18% compared to S1. Besides, the load cost index for S3 $VaR_{50\%}^{LC}$ is slightly higher than $VaR_{50\%}^{LC}$ for S5. This is because RTTR allows greater generation from cheaper units.

In terms of VLR and IVLR, both average values are lower under S6.

TABLE VIII
IEEE RTS NETWORK EVALUATION OF WIND FARMS & DR

Scenarios		S3	S7	S8
Reliability indices	EENS(MWh/day)	196	496	189
	EFI (int/day)	0.0383	0.0388	0.0383
	EDI*10 ⁻² (h/day)	23.31	23.8	23.19
Financial indices (k£)	VaR _{50%} ^{LC}	135.9	135.3	129.3
	VaR _{90%} ^{LC}	142.7	141.9	136.8
	VaR _{50%} ^{VLR}	1.6	-	1.05
	VaR _{50%} ^{IVLR}	2352	-	2268

We can note that DR provides the greatest benefits since all indices are drastically improved with DR, whilst benefits are only slightly higher under RTTR.

E. Impact of Wind Farms and DR on Network Reliability and Customer Costs & Revenues

In scenario S7, only wind farms are used, whilst scenario S8 uses DR in conjunction with wind farms. Table VIII shows that the more reliable and less expensive scenario is S8; the wind farms contribute to improving network reliability by 4% in EENS compared with S3 alone. Besides, a considerable reduction in EDI is achieved, whilst frequency of interruptions, EFI, remains the same as under S3. If compared with S1, wind farms alone (S7) improve network performance by 14% due to wind farms' network reinforcements. Also, VaR_{50%}^{LC} for S3 is slightly higher than VaR_{50%}^{LC} for S7 as wind farms are considered to have near-zero marginal costs. When wind farms are used in conjunction with DR (S8), this has the best effect on network performance and customer costs & revenues. This is because DR implementation helps when wind output is low and network components fail. Next, when wind output is high, spillage can occur as there is not enough capacity on the network to transfer the total amount of wind, thus leading to congestion when using STR for OHL operation. This can result in a small reduction of EENS.

VI. CONCLUSION

A probabilistic methodology for optimal scheduling of load reductions/recoveries in a day-ahead planning of transmission networks is proposed in the paper. The methodology recognizes several types of uncertainties, and finds optimal demand response scheduling using the network security and customer economics criteria. Impacts of wind generation and real-time thermal ratings of overhead lines are also studied.

The developed case studies have demonstrated that the value of optimal demand scheduling combined with real-time thermal ratings can be significant when using nodal marginal prices compared to using the hourly loads only. In particular, both reliability and financial metrics can be improved by a factor of around 66% for expected energy not served and around 5% for value at risk for costs of demand. Improvements in other reliability indicators and expected generation costs were also observed. Nonetheless, selection of the reliability indicator to base the operational decisions on demand scheduling can

be of highest importance; having multiple indices can therefore help system operators to make more informed decisions on 'best' demand response practice. As a final comment, the consistent use of a probabilistic approach to model various network uncertainties and variability of nodal marginal prices provides a superior analysis compared to traditional analytical techniques.

The future work considers inclusion of optimal energy storage scheduling to increase system reliability. Combined impact of energy storage, demand response and wind generation will be studied in greater detail.

REFERENCES

- P. Denholm and M. Hand, "Grid flexibility and storage required to achieve very high penetration of variable renewable electricity," *Energy Pol.*, vol. 39, no. 3, pp. 1817–1830, 2011.
- D. T. Nguyen, M. Negnevitsky, and M. de Groot, "Pool-based demand response exchange—Concept and modeling," *IEEE Trans. Power Syst.*, vol. 26, no. 3, pp. 1677–1685, Aug. 2011.
- A. S. Deese, E. Stein, B. Carrigan, and E. Klein, "Automation of residential load in power distribution systems with focus on demand response," *IET Gener. Transm. Distrib.*, vol. 7, no. 4, pp. 357–365, Apr. 2013.
- P. Wang, Y. Ding, and Y. Xiao, "Technique to evaluate nodal reliability indices and nodal prices of restructured power systems," *IEE Proc. Gener. Transm. Distrib.*, vol. 152, no. 3, pp. 390–396, May 2005.
- M. Fotuhi-Firuzabad and R. Billinton, "Impact of load management on composite system reliability evaluation short-term operating benefits," *IEEE Trans. Power Syst.*, vol. 15, no. 2, pp. 858–864, May 2000.
- E. Karangelos and F. Bouffard, "Towards full integration of demand-side resources in joint forward energy/reserve electricity markets," *IEEE Trans. Power Syst.*, vol. 27, no. 1, pp. 280–289, Feb. 2012.
- D. T. Nguyen, M. Negnevitsky, and M. de Groot, "Modeling load recovery impact for demand response applications," *IEEE Trans. Power Syst.*, vol. 28, no. 2, pp. 1216–1225, May 2013.
- N. Ruiz, I. Cobelo, and J. Oyarzabal, "A direct load control model for virtual power plant management," *IEEE Trans. Power Syst.*, vol. 24, no. 2, pp. 959–966, May 2009.
- A. Molina-Garcia, F. Bouffard, and D. S. Kirschen, "Decentralized demand-side contribution to primary frequency control," *IEEE Trans. Power Syst.*, vol. 26, no. 1, pp. 411–419, Feb. 2011.
- C. L. Su and D. Kirschen, "Quantifying the effect of demand response on electricity markets," *IEEE Trans. Power Syst.*, vol. 24, no. 3, pp. 1199–1207, Aug. 2009.
- R. Billinton and W. Li, *Reliability Assessment of Electrical Power Systems Using Monte Carlo Methods*. London, U.K.: Plenum, 1994.
- J. Schachter and P. Mancarella, "A short-term load forecasting model for demand response applications," in *Proc. IEEE 11th Int. Conf. Eur. Energy Market (EEM)*, Krakow, Poland, 2014, pp. 1–5.
- "The value of lost load (VoLL) for electricity in Great Britain: Final report for OFGEM and DECC," London Econ., London, U.K., Tech. Rep., 2013.
- Current Rating Guide for High Voltage Overhead Lines Operating in the UK Distribution System*, document ER. P27, Energy Netw. Assoc., London, U.K., 1986.
- IEEE Standard for Calculating the Current-Temperature of Bare Overhead Conductors*, IEEE Standard 738-2006, 2007, pp. 1–59.
- [Online]. Available: <http://badc.nerc.ac.uk/data/ukmo-midas/WPS.html>
- J. M. Arroyo and F. D. Galiana, "Energy and reserve pricing in security and network-constrained electricity markets," *IEEE Trans. Power Syst.*, vol. 20, no. 2, pp. 634–643, May 2005.
- M. S. Bazaraa, J. J. Jarvis, and H. D. Sherali, *Linear Programming and Network Flows*, 4th ed. Hoboken, NJ, USA: Wiley, 2010.
- I. J. Perez-Arriaga and C. Meseguer, "Wholesale marginal prices in competitive generation markets," *IEEE Trans. Power Syst.*, vol. 12, no. 2, pp. 710–717, May 1997.
- K. Singh, N. P. Padhy, and J. Sharma, "Influence of price responsive demand shifting bidding on congestion and LMP in pool-based day-ahead electricity markets," *IEEE Trans. Power Syst.*, vol. 26, no. 2, pp. 886–896, May 2011.
- X. Cheng and T. J. Overbye, "An energy reference bus independent LMP decomposition algorithm," *IEEE Trans. Power Syst.*, vol. 21, no. 3, pp. 1041–1049, Aug. 2006.

- 1081 [22] S. Wong and J. D. Fuller, "Pricing energy and reserves using stochastic
1082 optimization in an alternative electricity market," *IEEE Trans. Power*
1083 *Syst.*, vol. 22, no. 2, pp. 631–638, May 2007.
- 1084 [23] D. S. Kirschen, K. R. W. Bell, D. P. Nedic, D. Jayaweera, and
1085 R. N. Allan, "Computing the value of security," *IEE Proc. Gener.*
1086 *Transm. Distrib.*, vol. 150, no. 6, pp. 673–678, Nov. 2003.
- 1087 [24] G. Dorini, P. Pinson, and H. Madsen, "Chance-constrained optimization
1088 of demand response to price signals," *IEEE Trans. Smart Grid*, vol. 4,
1089 no. 4, pp. 2072–2080, Dec. 2013.
- 1090 [25] C. Chen, J. Wang, and S. Kishore, "A distributed direct load control
1091 approach for large-scale residential demand response," *IEEE Trans.*
1092 *Power Syst.*, vol. 29, no. 5, pp. 2219–2228, Sep. 2014.
- 1093 [26] A. Abdollahi, M. P. Moghaddam, M. Rashidinejad, and
1094 M. K. Sheikh-El-Eslami, "Investigation of economic and environmental-
1095 driven demand response measures incorporating UC," *IEEE Trans.*
1096 *Smart Grid*, vol. 3, no. 1, pp. 12–25, Mar. 2012.
- 1097 [27] M. H. Albadi and E. F. El-Saadany, "A summary of demand response
1098 in electricity markets," *Elect. Power Syst. Res.*, vol. 78, no. 11,
1099 pp. 1989–1996, 2008.
- 1100 [28] E. Agneholm and J. Daalder, "Load recovery in different industries fol-
1101 lowing an outage," *IEE Proc. Gener. Transm. Distrib.*, vol. 149, no. 1,
1102 pp. 76–82, Jan. 2002.
- 1103 [29] G. Strbac, E. D. Farmer, and B. J. Cory, "Framework for the incorpo-
1104 ration of demand-side in a competitive electricity market," *IEE Proc.*
1105 *Gener. Transm. Distrib.*, vol. 143, no. 3, pp. 232–237, May 1996.
- 1106 [30] "National grid EMR analytical report," Nat. Grid, Warwick, U.K., Tech.
1107 Rep., 2013.
- 1108 [31] A. Shapiro and S. Basak, "Value-at-risk based risk management: Optimal
1109 policies and asset prices," *Rev. Financ. Stud.*, vol. 14, no. 2, pp. 371–405,
1110 2001.
- 1111 [32] K. Kopsidas, S. M. Rowland, and B. Boumeceid, "A holistic method for
1112 conductor ampacity and sag computation on an OHL structure," *IEEE*
1113 *Trans. Power Del.*, vol. 27, no. 3, pp. 1047–1054, Jul. 2012.
- 1114 [33] P. Giorsetto and K. F. Utsurogi, "Development of a new procedure for
1115 reliability modeling of wind turbine generators," *IEEE Trans. Power*
1116 *App. Syst.*, vol. PAS-102, no. 1, pp. 134–143, Jan. 1983.
- 1117 [34] *Renewable Sources of Energy*, Dept. Energy Climate Change, Dig. U.K.
1118 Energy Stat., London, U.K., 2014, pp. 157–193.
- 1119 [35] K. Soren, M. Poul-Eric, and A. Shimon, *Wind Energy Implications of*
1120 *Large-Scale Deployment on the GB Electricity System*, Roy. Acad. Eng.,
1121 London, U.K., 2014, p. 72.
- 1122 [36] C. Fong *et al.*, "The IEEE reliability test system-1996. A report prepared
1123 by the reliability test system task force of the application of probabili-
1124 ty methods subcommittee," *IEEE Trans. Power Syst.*, vol. 14, no. 3,
1125 pp. 1010–1020, Aug. 1999.
- 1126 [37] R. D. Zimmerman, E. M.-S. Carlos, and D. Gan, *MATPOWER:*
1127 *A MATLAB Power System Simulation Package, Version 3.1b2, User's*
1128 *Manual*, Power Systems Eng. Res. Center, New York, NY, USA, 2011.



Manchester, with main research interests on plant modeling and reliability and adequacy.

1141



Alexandra Kapetanaki (S'12) received the M.Eng. degree in electrical engineering and computer science from the National Technical University of Athens, Greece, in 2011. She is currently pursuing the Ph.D. degree with the Electrical Energy and Power Systems Group.

Her current research interests include optimization of power system operation, stochastic modelling, risk management, and electricity markets.

1150



Victor Levi (S'89–M'91–SM'13) received the M.Sc. and Ph.D. degrees in electrical engineering from the University of Belgrade, Belgrade, Yugoslavia, in 1986 and 1991, respectively.

From 1982 to 2001, he was with the University of Novi Sad, Novi Sad, Yugoslavia, where he became a Full Professor in 2001. He was with the University of Manchester, Manchester, U.K., from 2001 to 2003, and then with United Utilities and Electricity North West from 2003 to 2013. In 2013, he rejoined the University of Manchester.

1161

AUTHOR QUERIES

AUTHOR PLEASE ANSWER ALL QUERIES

PLEASE NOTE: We cannot accept new source files as corrections for your paper. If possible, please annotate the PDF proof we have sent you with your corrections and upload it via the Author Gateway. Alternatively, you may send us your corrections in list format. You may also upload revised graphics via the Author Gateway.

AQ1: Please provide the author name, department name, and technical report number for References [13] and [30].

AQ2: Please verify and confirm the edits made to References [14], [34], [36], and [37] are correct as set.

AQ3: Please provide the title and accessed date for Reference [16].

IEEE PROOF